An Experimental Study of the Microwave Performance and Limitations of the Tektronix Discrete Prototype Heterojunction Bipolar Transistor (HBT)

James W. Mattern
B.S. Computer Engineering,
Portland State University, 1986

A thesis submitted to the faculty
of the Oregon Graduate Center
in partial fulfillment of the
requirements for the degree
Master of Science
in
Electrical Engineering

June, 1989

The thesis "An Experimental Study of the Microwave Performance and Limitations of the Tektronix Discrete Prototype Heterojunction Bipolor Transistor (HBT) ", by James W. Mattern has been examined and approved by the following Examination Committee.

Dr. V. S. Rao Gudimetla
Assistant Professor
Thesis Research Advisor

Dr. S. J. Prasad
Engineer, Tektronix

Mr. Tom Ruttan
Engineer, Tektronix

Dr. J. Fred Holmes
Professor

Dr. Dae Mann Kim
Professor

DEDICATION

To My Wife, Kathleen

ACKNOWLEDGEMENTS

I am very greatful to my thesis advisor, Dr. Rao Gudimetla for his wisdom and guidance in my work, both in this research and my education.

A special thanks to Dr. Carl Clawson. I am truly thankful for his insight and continuous encouragement. His knowledge of the physics of these devices was always very helpful and was extremely appreciated. He continuously challanged me to perform to my best ability.

Many of the pitfalls and traps that any "real-life" experiment will always bring forth were avoided with the help of Ed Knapp. I will always be grateful for his wisdom and patience.

I would also like to thank Tom Ruttan for his assistance, and all those people in the Microwave Technology Group for their guidance.

I will not forget the many hours that were spent with the entire Technology Group in the Solid State Research Labs (SSRL) at Tektronix.

I would like to thank my thesis committee, Dr. Rao Gudimetla, Dr. Jay Prasad, Dr. Fred Holmes, Dr. Dae Man Kim and Tom Ruttan for their hours spent and their many helpful suggestions in this effort.

I thank my family for all the support that they have given me these six and a half years of education. Thanks go to my wife, Kathleen for being there and understanding. And a special thanks to Jessica and Lindsey for their love and patience while their daddy was away.

Finally, I must acknowledge the Lord Jesus Christ who has always provided the ultimate guidance.

CONTENTS

LIST OF FIGURES AND TABLES

ABSTRACT

An Experimental Study of the Microwave Performance and Limitations of the Tektronix Discrete Prototype Heterojunction Bipolar Transistor (HBT)

James W. Mattern, M.S.
Oregon Graduate Center, 1989

Supervising Professor: V. S. Rao Gudimetla

This report will show that the hybrid-π model representing the operation of simple bipolar transistors is an adequate model for the Heterojunction Bipolar Transistor. The equivalent circuit model based on the hybrid-π model, will be first, estimated from the physics of the device, tuned by analysis of microwave data from 45 MHz to 15 GHz and finally optimized to extract the individual circuit elements described by the hybrid-π model. The model will show that the element parameters of the HBT structure can be extracted from the microwave S parameter data.

INTRODUCTION

In the Spring of 1988, Dr. Clawson, Dr. Gudimetla, Dr. Prasad and I met to discuss a mutual need. Tektronix Solid State Research Laborotory needed a Graduate Student to provide microwave measurements and characterization of the TEK discrete prototype HBT device; I required an experimentally based thesis.

To meet these requirements, this work shows the results of the experimental microwave measurements and characterization of the HBT. This work includes the algorithm needed to develop the equivalent circuit model of any transistor.

Chapter 1, consists of the basics of understanding the operation of transistors in general and of the unique operation of the HBT. Chapter 2, covers the collection and analysis of the microwave data. A discussion of the optimization of the circuit model and limitations of optimization are in chapter 3. Chapter 4, discusses the resulting circuit file. Suggestions for improving the fabrication and performance of the HBT is covered in chapter 5. And finally, a few brief conclusions, are in chapter 6.

CHAPTER 1: BASICS OF THE HBT

There exist many types of bipolar transistors on the market today. The most commonly known of these is the silicon npn homojunction transistor. It is fairly easy to find one that operates above 500 MHz. The current trend in the electronics industry is designing circuits that operate above 1GHz. This creates very high demand for a device that provides transistor operation well into the GHz range. A designer may even be quoted as saying that they need a device that will operate from "DC to Daylight".

A heterojunction can be defined as the interface between two dissimilar [1] materials. For this work, the HBT is defined as a transistor structure that consists of an emitter-base junction made up of two different monocrystalline semiconductor materials: that is, GaAs and GaAlAs.

The theory of the Heterojunction Bipolar Transistor(HBT) was first claimed by William Shockley in his 1951 patent. The attempt to understand the operation and manufacture of the HBT did not actually begin to occur until it was suggested by Herbert Kroemer. [2-4]

Kroemer suggested that very high injection efficiencies may be obtained by HBT structures compared to the homojunction transistors. Higher injection efficiencies imply higher gain. The need for this type of technology for microwave circuitry is very desirable. Microwave transistors have been designed and modeled earlier by M. H. White [5] and Harry Cooke. [6] These works form the basis for any characterization and modeling of microwave devices.

The attempts to understand and manufacture HBT structures has yielded many different [7] topologies, found in the literature. The Rockwell HBT [8] structure shown in Figure 1.1 was chosen as the basis for the research at TEK. This mesa or island type structure is only one of many variations that can be found.

The advantages to this structure are high injection efficiency, making the device speed potentially very fast, the switching characteristics can be controlled by epitaxial deposition, i.e. the electrical and mechanical characteristics of each grown layer can be predetermined with great accuracy and also, the 1/f noise of this [9] device can be very low compared to FETs.

A disadvantage of this structure is the collector down discrete process. Therefore, no circuits may be designed on the wafer. Also, since this technology is immature, epitaxial material comes at a very high cost.

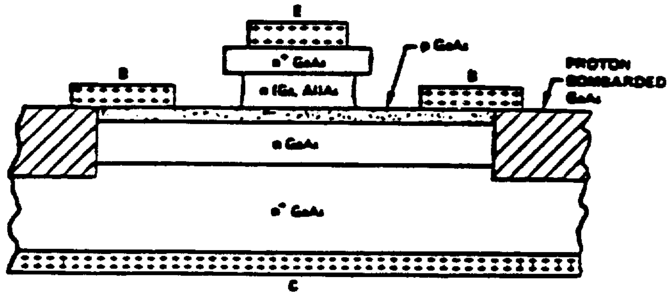

Rockwell mesa HBT [Asbeck 1982c]			
	Al fraction	Doping(cm^{-3})	Thickness(μm)
Cap	0	2×10^{18}(Si)	0.2
Emitter	0.3	5×10^{17}(Si)	0.25
Base	0	1×10^{19}(Be)	0.05
Collector	0	5×10^{16}(Si)	0.5
Substrate	0	2×10^{18}(Si)	

• Material:	AlGaAs/GaAs
• n-type contact:	Au/Ge/Ni
• p-type contact:	Zn/Au
• Isolation:	proton implant
• $\rho_{\square B}$:	800 $\Omega/\square$
• r_B:	13 Ω
• Emitter size:	5 $\mu m \times 20\ \mu m \times 5$ fingers
• β:	40-120
• f_T:	11 GHz at $J_E = 1.6\times10^4 A/cm^2$
• f_{max}:	4-5 GHz
• Offset voltage:	0.5 V

Figure 1.1. The Rockwell mesa HBT

1.1 Transistor Operation

Kromer predicted very high injection efficiency in the HBT. To show this, examine the operation of the transistor.

Terminal currents and the internal currents are shown [10] in Figure 1.2 with the convention of the current flowing into the device as positive. The internal currents flowing in the +x direction are positive. Therefore I_n, I_p and I_r are negative, normally I_E is negative with I_C and I_B positive. The components of interest at this point are:

I_E	Total Emitter Current
I_B	Total Base Current
I_C	Total Collector Current
I_n	Electron current injected into the base
I_p	Hole current injected into the emitter
I_r	Recombination current in the base

The terminal currents can be expressed in terms of the internal currents as:

$$I_E = I_p + I_n \tag{1.1a}$$

$$I_B = -I_p - I_r \tag{1.1b}$$

$$I_C = -I_n + I_r \tag{1.1c}$$

The most common parameter of any bipolar transistor is common emitter current gain defined as:

$$\beta = \frac{I_C}{I_B} \tag{1.2}$$

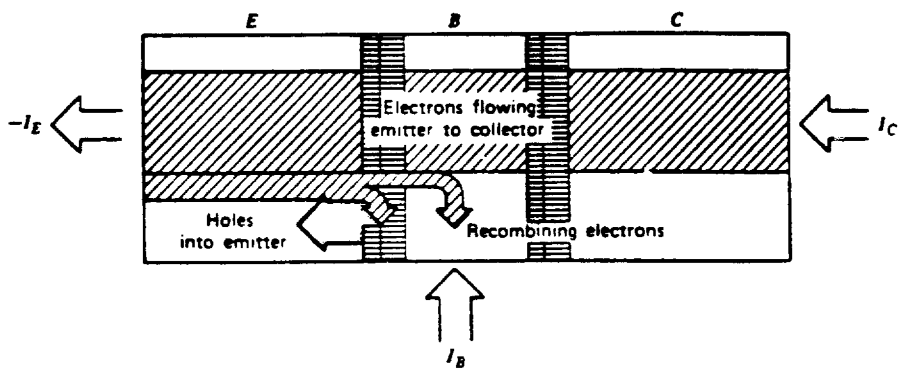

Figure 1.2. Transistor Current Flow

The common base current gain [11] is defined by:

$$\alpha = -\frac{I_C}{I_E} = \frac{I_n - I_r}{I_p + I_n} \tag{1.3a}$$

$$\alpha = \left[\frac{I_n}{I_p + I_n}\right]\left[\frac{I_n - I_r}{I_n}\right] \tag{1.3b}$$

The first expression on the right of equation 1.3b is the emitter efficiency:

$$\gamma = \frac{I_n}{I_p + I_n} \tag{1.4}$$

The right side expression is the base transport factor:

$$\alpha_T = \frac{I_n - I_r}{I_n} \tag{1.5}$$

These gain expressions, β and α are related to each other by the relationship:

$$\beta = \frac{\alpha}{1-\alpha} \tag{1.6}$$

The parameter α can easily be related to internal current component factors: [11]

$$\alpha = \gamma\alpha_T \tag{1.7}$$

This shows that β is a function of emitter efficiency (γ), which is the ratio of the injected electron current to the total emitter current; and the base transport factor (α_T), which is the ratio of collector current to the injected electron current. For any transistor to have high β, both of these terms need to be close to unity. [11]

We wish to establish the influence of the emitter and base properties on current gain with simple mathematics. To do so, the following is assumed:

1. The emitter-base is forward biased such that the minority carrier densities exceed their equilibrium values, i.e. $V_{BE} >> V_T$.

2. The collector-base junction is reverse biased such that the minority carrier density in the collector junction is far below the equlibrium value. This neglects recombination in the emitter.

3. The emitter width W_E is much less than the hole diffusion length, L_{pE}, to neglect the recombination in the emitter. [12, 13]

With these assumptions in place the equations for the internal currents have been described by Muller and also Clawson and are summarized here:

$$I_p = -q\frac{A_E\, n_i^2\, D_{pE}}{N_{dE}\, W_E}\; e^{\frac{V_{BE}}{V_T}} \tag{1.8}$$

$$I_n = -q\frac{A_E\, n_i^2\, D_{nB}}{N_{aB}\, W_B}\; e^{\frac{V_{BE}}{V_T}} \tag{1.9}$$

$$I_r \approx -q\frac{A_E\, n_i^2\, D_{nB} W_B}{2N_{aB} L_{nB}^2}\; e^{\frac{V_{BE}}{V_T}} \tag{1.10a}$$

The recombination current can be approximated by:

$$I_r \approx \frac{W_B^2}{2L_{nB}^2} I_n \qquad (1.10b)$$

With these expressions and some manipulation, emitter efficiency becomes:

$$\gamma \approx 1 - \frac{D_{pE} N_{aB} W_B}{D_{nB} N_{dE} W_E} \qquad (1.11)$$

where γ is assumed to be close to unity. From tables and charts in Sze, it is found that D_{pE} and D_{nB}, are of the same order of magnitude. The parameters W_B and W_E can also be assumed to be within the same order of magnitude. This means then that the condition, $N_{dE} >> N_{aB}$, must be met for γ to be close to one and yield high current gain (β).

The base transport factor provides the clue for the second requirement. It can be determined by the combination of equations 1.5 and 1.10b.

$$\alpha_T \approx 1 - \frac{W_B^2}{2 L_{nB}^2} \qquad (1.12)$$

Thus, the second requirement is that $W_B << L_{nB}$.

Thus high gain can be achieved by lightly doping the base and heavily doping the emitter. Further analysis reveals the limitation with homojunction transistors. The equation for gain is:

$$\beta \approx \frac{N_{dE} W_E D_{nB}}{N_{aB} W_B D_{pE}} \qquad (1.13)$$

The degrees of freedom to increase the d.c. gain is limited to the thickness of the base (W_B), the doping level in the emitter (N_{dE}), and the doping level in the base, (N_{aB}). This equation shows the inherent limitation of the highly doped emitter, and the thin base. These elements control the requirements for d.c. operation which conflict with the microwave performance.

In the Heterojunction Bipolar Transistor (HBT), the degrees of freedom, include those of the homojunction and an additional exponential factor. The expression for emitter efficiency is:

$$\gamma = 1 - \frac{D_{pE}\, N_{aB}\, W_B}{D_{nB}\, N_{dE}\, W_E} \exp\left(-\frac{\Delta E_g}{kT} \right) \tag{1.14}$$

This exponential factor limits the deviation from unity of γ to be very small. Provided the base transport factor is near unity, the emitter efficiency continues to be the dominant factor in β. The current gain, β, is proportional to $\exp(\Delta E_g / kT)$. Therefore, to produce very large gain in a transistor, a large difference in energy gap between the materials at the junction will create an exponential [2] gain possibility. This is the basic principle of the wide-gap emitter proposed by Kroemer.

This additional exponential freedom allows the theory to predict gain exceeding 100,000. Most applications do not require large d.c. gain. This extremely large gain can be sacrificed for speed enhancements by lowering the emitter doping level. This will cause a decrease the emitter capacitance. By increasing the base doping level, the base resistance is lowered. The lower emitter capacitance and lower base resistance directly lower the RC time constants of the junctions and increase the device frequency of operation.

1.2 Hybrid-π Model of the HBT

The basis of the HBT effort is to substitute the homojunction transistor. Therefore, it is expected to meet similiar performance measures. The figures of merit for the HBT are then identical to those for any bipolar transistor. The equivalent circuit for the HBT using the standard hybrid-π model is shown in Figure 1.3. Each element in the model can be derived from basic semiconductor physics. The circuit model is the familiar linearized Ebers-Moll [14] model. The distributed base series resistance r_b will be additionally modeled as lumped elements [15] in a transmission line.

The hybrid-π model allows the determination of each element in the transistor assuming a set bias point, directly from the physical layout and the doping levels of the device. Figure 1.3, shows the typical equivalent circuit found in many text books. We will show how each element is determined.

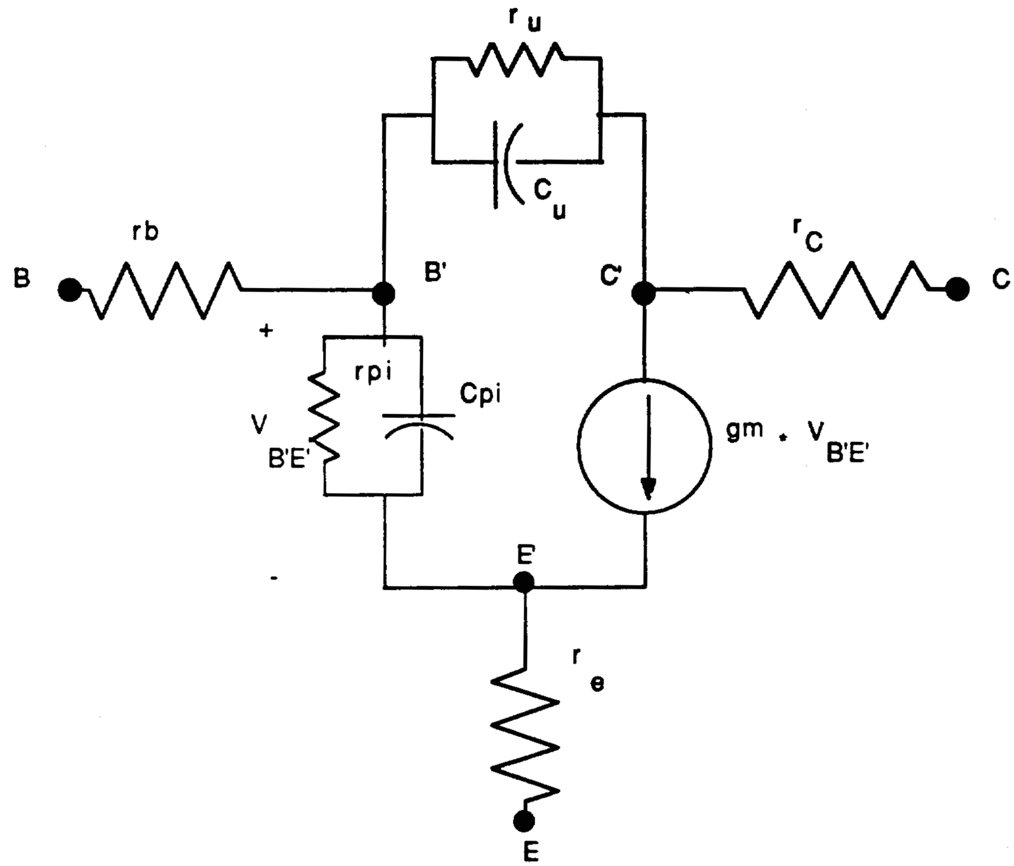

Figure 1.3. The hybrid-π model of the bipolar transistor.

1.3 Base Resistance

The base resistance can be divided into three regional elements:

$$r_b = r_{bi} + r_{bx} + r_{bc} \tag{1.15}$$

The intrinsic base resistance, r_{bi}, is the resistance directly under the emitter. The parameter r_{bx} is the extrinsic base resistance between the emitter and the base contact and r_{bc} is the resistance due to the base contact. This is illustrated [16] by Figure 1.4.

The formula for double-sided contact geometry, where a single emitter finger is sandwiched between two base fingers is: [13]

$$r_{bi} = \frac{\rho_{IB} S_E}{12 L_E} \tag{1.16}$$

S_E is defined as the stripe width of the emitter, and L_E is the emitter stripe length.

The extrinsic base resistance:

$$r_{bx} = \frac{\rho_{XB} X_{EB}}{2 L_E} \tag{1.17}$$

here, X_{EB} is the spacing between the emitter and base electrodes and ρ_{XB} is the sheet resistance of the extrinsic base in $\Omega / \square$.

We find in the work by Reeves and Harrison, the base contact resistance: [17]

$$r_{bc} = \frac{\rho_{sk} L_T}{2L_E} \coth\left[S_b / L_T \right] \tag{1.18}$$

where S_b is the width of the base stripe, and L_T is the transfer length of the current flowing laterally under the contact.

The sheet resistance under the base contact, ρ_{sk} is estimated to be nearly equal to ρ_{XB} for the mesa-etch devices. [18] L_T is given to be: [19]

$$L_T{}^2 = \frac{\rho_{cp}}{\rho_{sk}} \tag{1.19}$$

The sum of these three resistances is the total base resistance, r_b.

The interdigitated device, FINT, as shown in Figure 1.5, which is of interest in this work, has 5 emitter fingers and 6 base fingers.

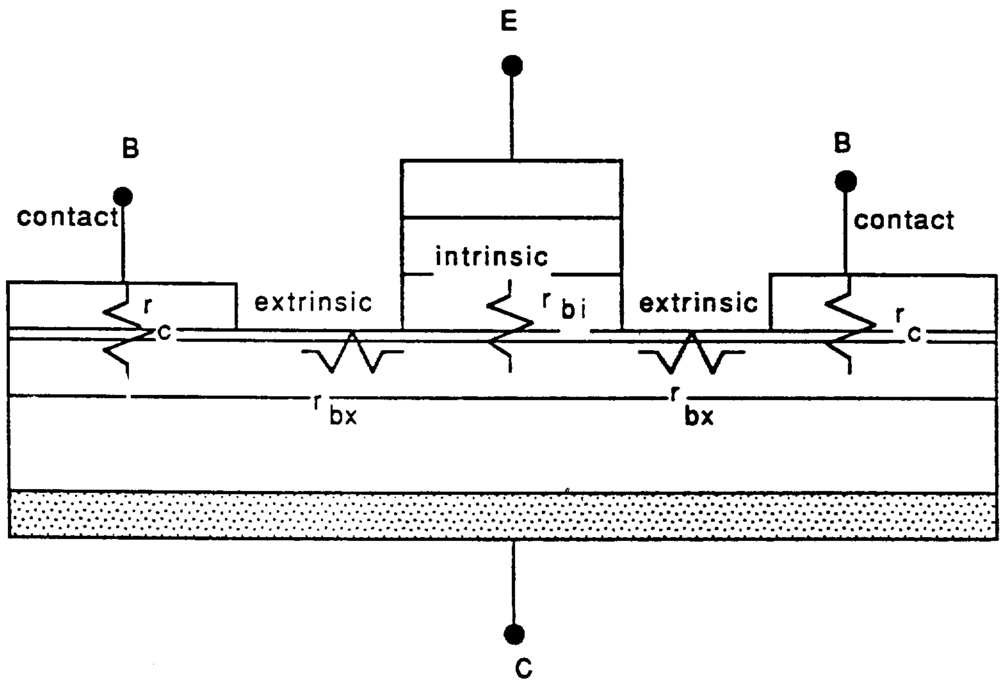

Figure 1.4. The Three Basic Components of the Distributed Base Resistance

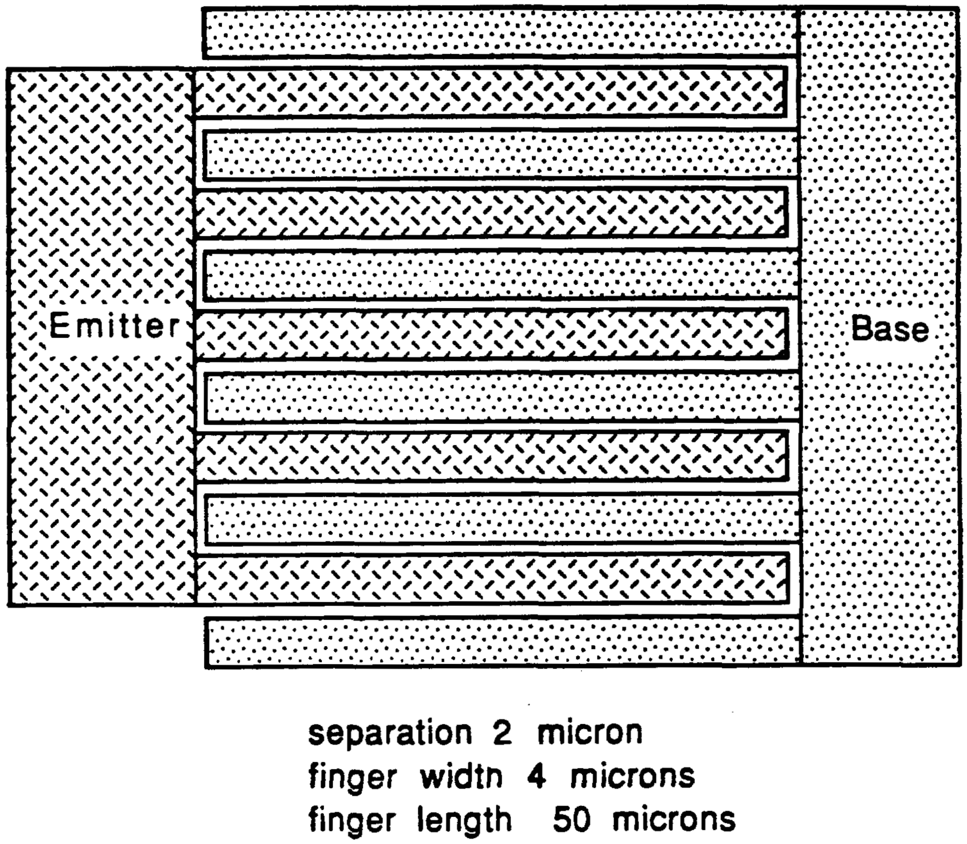

Figure 1.5. Layout of the FINT

This yields 5 resistive elements of each regional component in parallel with like regional components.

The formula for r_μ, the Early effect resistance, is described by: [10]

$$r_\mu = \frac{\beta_0 V_A}{g_m V_T} \tag{1.20}$$

Since the Early voltage (V_A), may be assumed to be larger than thermal voltage, $V_A >> V_T$, a very high value for r_μ is obtained and at the frequencies of interest, $r_\mu >> 1/\omega C_\mu$.

The dynamic resistance between the emitter and the base is given by Muller and Kamins:

$$r_\pi = \frac{\beta_0}{g_m} \tag{1.21}$$

The parameter β_o is the d.c. current gain.

The sum of the emitter-base junction capacitance, C_{jE}, and the diffusion capacitance, C_D is known as C_π.

$$C_\pi = C_{jE} + C_D \tag{1.22}$$

where

$$C_D = g_m \tau_f \tag{1.23}$$

and the vertical forward charging time in the device is:

$$\tau_f = \frac{\partial Q}{\partial I_C} \tag{1.24}$$

where Q is the minority carrier stored charge in the device. C_μ is the sum of the collector-base capacitance, C_{jC} and an Early effect adjustment term:

$$C_\mu = C_{jC} + \frac{V_T}{V_A} C_D \tag{1.25}$$

Finally, the transconductance of the device g_m is given by:

$$g_m = \frac{dI_C}{dV_F} = \frac{I_C}{V_T} \tag{1.26}$$

Here V_F is the forward voltage across the internal base and emitter nodes B' and E' in Figure 1.3.

1.4 Charging Times in the HBT

The forward transit time for different regions:

$$\tau_f = \tau_e + \tau_b + \tau_c' \tag{1.27}$$

The charging time of the quasi-neutral emitter is τ_e, τ_b is the base charging time, and τ_c' is the charging time of the collector-base space charge region. The charging time of the emitter space charge region and the charge stored in the neutral collector are assumed to be zero. The individual regional components are modeled by:

$$\tau_e = \frac{W_E^2}{2D_{pE}}(1-\gamma) \tag{1.28}$$

and

$$\tau_c' = \frac{d_C}{2v_s} \tag{1.29}$$

where d_C is the width of the collector-base space charge region, and $v_s \approx 2 \times 10^7$ cm / s as estimated in Muller and Kamins is defined as the steady-state saturation velocity of GaAs. From the work by M. Das, [15] the equation for the base time constant is:

$$\tau_b = \frac{W_B^2}{2D_{nB}} + \frac{W_B}{v_s} \tag{1.30}$$

It is interesting to examine transit time from the collector to emitter and how these parameters can be applied to determine f_T and $f_{\max}$. The total transit time between collector and emitter can be expressed as:

$$\tau_T = \frac{C_\pi + C_\mu}{g_m} + C_\mu (r_c + r_e) \tag{1.31}$$

Substituting,

$$C_\pi = C_{jE} + C_D \tag{1.32}$$

$$C_\mu = C_{jC} + \frac{V_T}{V_A} C_D \tag{1.33}$$

and assuming that $V_A >> V_T$, noting that

$$C_D = g_m \tau_f \tag{1.34}$$

equation 1.26 then becomes:

$$\tau_T = \tau_f + \frac{C_{jE} + C_{jC}}{g_m} + C_{jC} (r_e + r_C) \tag{1.35}$$

where τ_f is the vertical forward charging time.

The junction capacitances can be modeled standard formula, $C = \varepsilon A / d$, where A is the junction area and d the depletion layer thickness with ε the dielectric constant.

The depletion layer is defined [10] as:

$$d = \left(\frac{2 \varepsilon_s V_J}{qN} \right)^{1/2} \tag{1.36}$$

This equation applies to junctions with one side of the junction very heavily doped and the other, N in the equation, is the doping concentration of the lightly doped side.

The emitter resistance can be separated into the contribution due to the n-ohmic contact and the bulk semiconductor region as:

$$r_e\,(\text{contact}) = \frac{\rho_{cn}}{A_E} \tag{1.37}$$

$$r_e\,(\text{bulk}) = \frac{\rho_{E1} W_{E1} + \rho_{E2} W_{E2}}{A_E} \tag{1.38}$$

The collector resistance is:

$$r_c = \frac{\rho_c}{A_E}(d_c - W_c) \tag{1.39}$$

The value of τ_T can now be estimated and some theoretical predictions can be made for f_T and $f_{\max}$ via the relations:

$$f_T = (2\pi\tau_T)^{-1} \tag{1.40}$$

and

$$f_{\max} = \left[\frac{f_T}{8\pi r_b C_{jC}}\right]^{1/2} \tag{1.41}$$

The figure of merit f_T is commonly defined as the frequency at which the common-emitter current gain becomes unity or extrapolates to zero when current gain expressed in dB, is plotted against log frequency. The other important high frequency parameter is $f_{\max}$. This is the frequency which the Maximum Available Gain(*MAG*) becomes unity or a semi-log plot extrapolates to zero. MAG is the ratio of power available from the network to the power available from the source when the input and output ports are properly matched.

It is appropriate to point out that the wafers were purchased from various vendors for this project. Our goal was to fabricate usable devices from these wafers.

1.5 Problems Encountered in Computer Estimation and Data Available

Using these formulas and other constraints, found in basic semiconductor physics literature, a computer program was written to analyze the FINT devices. This analysis was limited by the data provided by run sheets describing the specifications of the process parameters. However, this analysis is intended only to provide a good starting point for further computer optimization. To facilitate this, assumptions on the missing or unverified data were made. Data for resistivities for run 189 were assumed to be the same as 186. Likewise, resistivities for runs 210-4 and 211-1b were assumed to be the same as the last available data from run 210-1.

These assumptions may over-estimate the parameters but will serve as a starting point for reference.

The parameter, β, and points for d.c. biasing were derived from I-V curves. Figure 1.6 illustrates the typical I-V curves encountered.

To be consistent with previous work conducted by Dr. Clawson, devices were chosen to be analyzed at 3 volts and swing current steps from 2 milliamps to 50 milliamps, re-examine the device on the curve-tracer, and then try to extend the analysis to 150 milliamps. Not many devices made the transition as problems may have created hot spots that destroyed the devices after only small bias swings. FINT devices of the dimensions noted earlier are capable of 400-500 milliamps. This limited the performance analysis of the device.

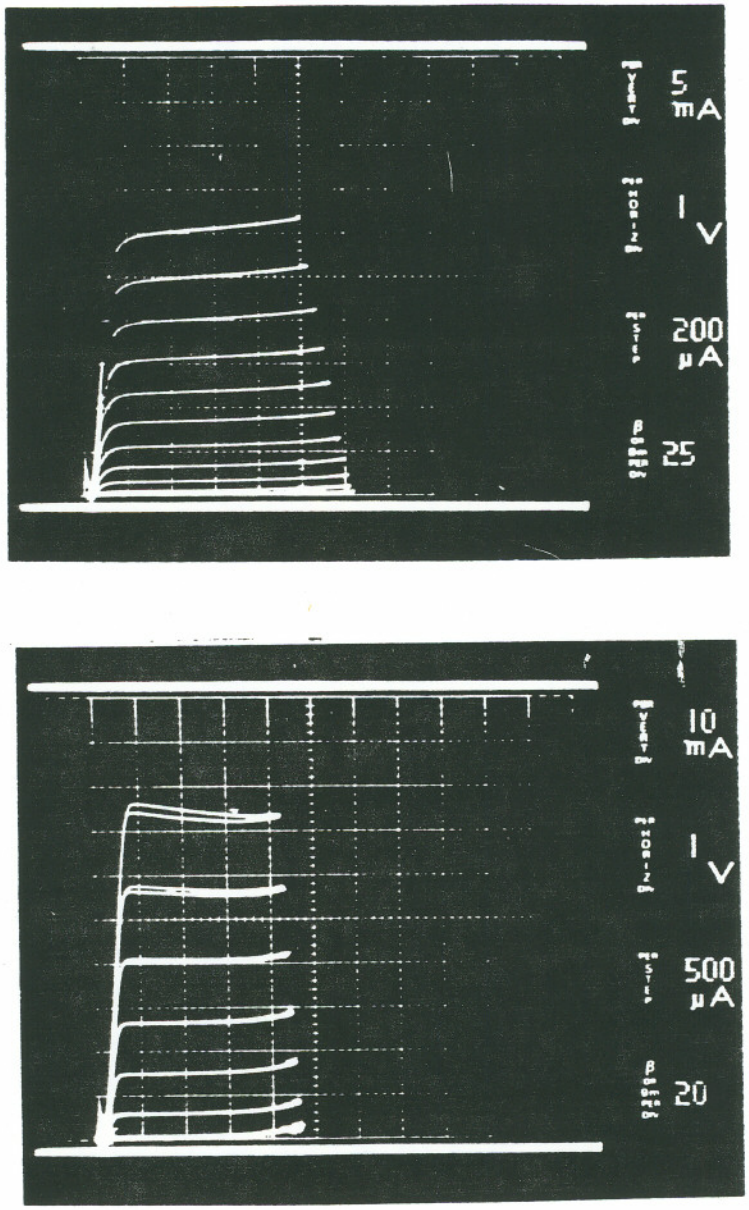

Figure 1.6. FINT I-V curves

Table 1.1 is a list of the common FINT parameters needed by the above equations for each run. Most are directly taken from reports internal to Tektronix. The resistivities for run 189-3 are assumed to be identical to run 186-2. Also run 210-4 and 211-1b have the same assumptions based on the incomplete data from 210-1. Table 1.2 shows the compilation of the computer results for runs 136-1, 136-2, 163-1, 186-2, 189-3, 210-1, 210-4, and 211-1b, a half wafer. A sample listing of the program can be found in Appendix C. Here, β is estimated from I-V curves and g_m is calculated based on earlier analysis. The parameters for the distributed base resistances are calculated separately and then added for r_b total. The calculated and tabulated results for f_T and $f_{\max}$ can be seen in Table 1.2. The results for f_T show that the device can run very fast with no changes. Theory does not include processing variables. The performance of $f_{\max}$ is not good which is a direct reflection of the high base resistances calculated by the computer with the asumptions mentioned. Obviously, those assumptions are far from the truth but the intent was to give the optimization program a good initial start.

The parameter, f_T, is also sensitive to changes to bias conditions. If the device could be biased to a higher voltage and current level, the performance should improve. The vertical time constant of the wafer, τ_f, directly influences the magnitude of f_T. It is initially possible the device is limited to 28 GHz by the doping profiles.

The possible effects of the parasitic pad capacitances, can be seen by examination of the last five lines of Table 1.2. This illustrates the effect of the physical layout of the launching microstrip structure. The layout of the microstrip lines to the device can effect device performance. The pad capacitances can dominate the performace of these devices.

COMMON DEVICE PHYSICAL PARAMETERS							
PARM	136	163-1	186-2	189-3	210-1	210-4	211-1b
$W_{e(um)}$	0.475	0.475	0.475	0.475	0.475	0.475	0.475
$W_{e1(um)}$	0.125	0.125	0.125	0.125	0.125	0.125	0.125
$W_{e2(um)}$	0.25	0.25	0.25	0.25	0.25	0.25	0.25
$W_{b(um)}$	0.1	0.1	0.1	0.1	0.1	0.1	0.1
$W_{c(um)}$	0.7	0.7	0.7	0.7	0.7	0.7	0.7
D_{pe}	5	5	5	5	5	5	5
D_{nb}	50	50	50	50	50	50	50
μ_{pe}	200	200	200	200	200	200	200
μ_{nb}	2000	2000	2000	2000	2000	2000	2000
N_{de}	5e17	5e17	5e17	5e17	9e17	9e17	6e17
N_{ab}	1e18	3e18	1e19	1e19	4e18	4e18	3.5e18
N_{dc}	5e16	3e16	9e16	3e16	2e17	1.6e16	1.6e16
ρ_{E1}	4e-3	4e-3	4e-3	4e-3	2.3e-3	2.3e-3	2.3e-3
ρ_{E2}	6.25e-3	6.25e-3	6.25e-3	6.25e-3	6.25e-3	6.25e-3	6.25e-3
ρ_{IB}	175	137	1180	1180	5e3	5e3	5e3
ρ_{X3}	300	300	991	991	5e3	5e3	5e3
ρ_{C}	6e-2	6e-2	6e-2	6e-2	6e-2	6e-2	6e-2
ρ_{Cn}	1e-6	1e-6	1e-6	1e-6	1e-6	1e-6	1e-6
ρ_{Cp}	5e-6	1e-3	5e-6	8e-6	6e-3	3e-3	6e-3
ρ_{SK}	600	600	1982	1982	1e3	1e3	1e3
A_e	1000	1000	1000	1000	1000	1000	1000
A_c	4158	4158	4158	4158	4158	4158	4158
$L_{e(um)}$	50	50	50	50	50	50	50
$L_{t(um)}$	0.91	12.91	0.5	0.64	7.75	7.75	7.75
$S_{b(um)}$	4	4	4	4	4	4	4
$S_{e(um)}$	4	4	4	4	4	4	4
$X_{eb(um)}$	2	2	2	2	1	1	2

Table 1.1 The Common Device Parameters.

COMPUTER ANALYSIS OF HBT FROM PHYSICAL PARAMETERS							
PARM	136	163-1	186-2	189-3	210-1	210-4	211-1b
$Beta$	100	45	50	40	50	25	20
$I_{C(ma)}$	50	50	50	50	50	50	50
$V_{CE(V)}$	3	3	3	3	3	3	3
g_m	1.93	1.93	1.93	1.93	1.93	1.93	1.93
Δ_{Ec}	0.15	0.15	0.187	0.187	0.187	0.187	0.187
$C_{jc(pf)}$	1.64	1.27	2.20	1.27	3.29	2.94	2.94
$C_{je(pf)}$	3.95	3.95	3.95	3.95	5.30	5.30	4.32
$r_{ec(ohm)}$	0.10	0.1	0.1	0.12	0.1	0.1	0.1
$r_{ebulk(ohm)}$	0.021	0.031	0.021	0.021	0.019	0.019	0.019
$r_{e(ohm)}$	0.12	0.12	0.12	0.12	0.12	0.12	0.12
$r_{c(ohm)}$	0.12	0.12	0.12	0.12	0.12	0.12	0.12
$r_{bi(ohm)}$	0.23	0.18	1.57	1.57	6.67	6.67	6.67
$r_{bx(ohm)}$	1.20	1.20	3.96	3.96	10.0	10.0	20.0
$r_{bc(ohm)}$	1.10	51.59	1.99	2.52	326	326	326
$r_{b(ohm)}$	2.53	52.97	7.53	8.06	342	342	352
$\tau_{f(ps)}$	2.27	2.54	2.12	2.52	1.89	1.92	1.93
$\tau_{T(ps)}$	5.56	5.55	5.83	5.53	7.11	6.88	6.40
$F_{max(GHz)}$	16.6	4.1	8.1	10.6	0.9	1.0	1.0
$F_{T(GHz)}$	28.6	28.7	27.3	28.8	22.4	23.1	24.9
$C_{pad(pf)}$	0.6	0.6	2.1	2.1	0.3	0.2	0.35
With C_{pad}							
$F_{max(GHz)}$	13.6	3.3	5.1	5.7	0.8	0.9	0.9
$F_{T(GHz)}$	26.5	26.5	21.4	22.3	21.7	22.6	23.9

Table 1.2 The Computer Modeled Data.

CHAPTER 2: DEVICE MEASUREMENTS

2.1 Measurement Test Set-Up

The completed HBT wafers were analyzed for d.c. performance parameters [6] and after verifing the performance, the devices were selected for microwave probing. Fingered devices consistently survived the fabrication process. A few of these were selected from each wafer. The wafers were then diced, and die-attached with gold epoxy, and wedge bonded to a preselected test hybrid structure.

Sweeping collector current in steps around a selected collector-emitter voltage allows the analysis of f_T vs I_C. Many of the FINT devices were chosen to be tested at 3 to 4 volts. Higher voltages were avoided to prevent catastrophic failure of the device.

The Hewlett-Packard HP8510a Automatic Network Analyzer [20] was used to extract S parameters via microwave ground-signal probes. Due to the orientation of the die on the hybrid substrate, and the launching pattern on the hybrid, the device was measured in the common-collector, emitter port 1 , base port 2 mode. The general test layout is shown in Figure 2.1.

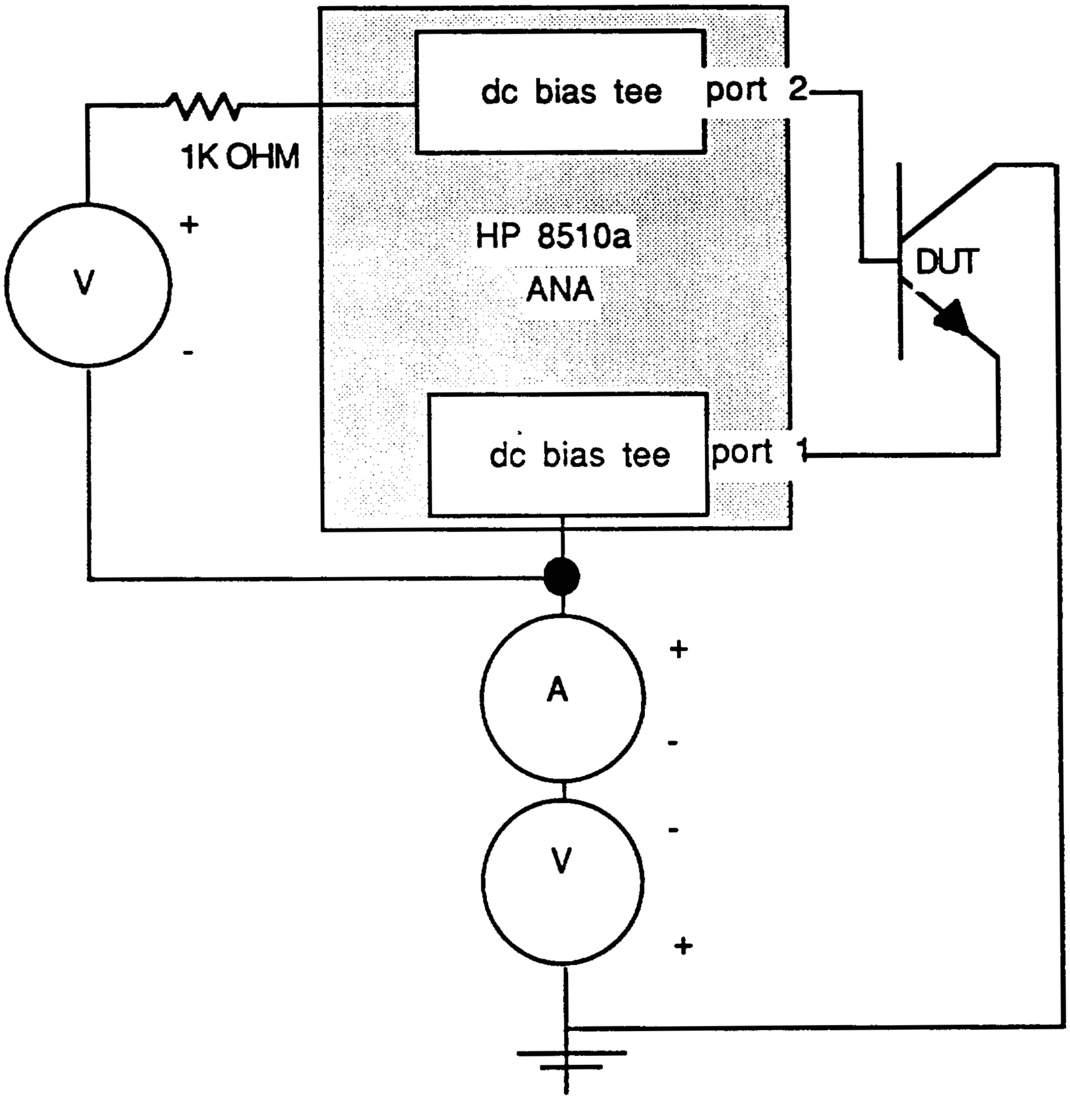

Figure 2.1. The Test Set-Up.

2.2 Calibration

When measurements are taken, the data collected includes information about the response of the test ports, [21,22] the test cables, the test probes, the test substrate, the bond wires and bond pads, and also the launching microstrip. Somewhere embedded in this data is the response of the device under test (DUT). In order to isolate the performance of the DUT from the rest of the network, de-embedding [23,24] or extraction of the DUT is necessary. This involves testing and storing the response of several devices within the memory of the HP8510, for mathematical removal from the data. This is calibration [25-27] or normalization of the measurements.

A separate hybrid was bonded with wire bonds of similar lengths and orientation to simulate the measurement plane near the device. Because the calibration substrate was a general design, the bond pads of the device were not calibrated out of the measurements. Terminations, shorts, opens and thru standards were available on the hybrid, thus the plane of the device bonding pads were estimated. If the effects of the bonding pads and lauching strip are to be removed from the collected data, calibration structures would have been needed to be fabricated on the wafer of the device.

There are errors resulting from the differences in the length of the wire bonds of the calibration substrate and the test hybrid. These errors, due to the bond wires, were then modeled as inductors to compensate.

The HP8510a is calibrated using the calibration substrate mentioned. This substrate defines the short, open and 50 ohm load refererence points for the internal software of the network analyzer.

Once the calibration routine had been performed, quick checks were made with the standards themselves. The purpose was to validate the calibration. For example, the 50 ohm load defines the center of the Smith-Chart. Measuring this device after calibration should show a single point at the center of the chart. Similar tests involving the short and open should also be done to verify that the short standard defines a point on the left edge and the open measurement defines a small arch on the right edge, center-line of the Smith-Chart. The arch is due to the fact that the open by definition has infinite impedance, yet for this measurement has some finite value. If these quick checks fail, the calibration needed to be repeated.

2.3 Device Data Collection

Data is collected automaticaly by an IBM controller for the HP 8510 ANA using GPIB bus. The program controls the HP8510 measurement routines, extracts the data and places it in the specified storage media. Tektronix supplied microwave probes were used to launch the microwave signals and collect the data. Each bias point is stepped thru the selected number of frequency points in the range of interest. To be consistent with prior work, 201 points over 45 MHz to 15 GHZ were collected for most of the devices. This data was then ported to a mainframe computing system for analysis. Data was analyzed by SUPER-COMPACT CAD tools, [28] and by SIM, a computer program written by the author, using techniques and formulas outlined by Gupta [29] and Gonzalez, for f_T and $f_{\max}$. An example of typical data collected and used throughout this work is shown in Table 2.1.

Super-Compact compatible S-Parameter data file								
k3v50ma 0.0450 15.0000 201 50 1								
run 210-1 #1 FINT								
vce 3v ie 50ma								
jim mattern 10/8/88								
	S11	S11	S21	S21	S12	S12	S22	S22
Freq	MAG	ANGLE	MAG	ANGLE	MAG	ANGLE	MAG	ANGLE
0.0450	0.8208	179.6	0.0481	3.3	1.8336	-2.4	0.9491	-3.3
0.6432	0.7853	173.2	0.0710	20.9	1.6056	-31.5	0.9284	-44.5
1.3910	0.7307	171.4	0.0982	13.1	1.1963	-57.0	0.9153	-82.5
1.9891	0.6954	171.6	0.1094	3.3	0.9500	-70.9	0.9261	-102.4
2.5874	0.6793	174.5	0.1128	-5.1	0.7776	-81.3	0.9306	-115.9
3.1856	0.6658	175.3	0.1146	-11.7	0.6557	-90.4	0.9380	-126.8
3.7838	0.6538	176.5	0.1171	-18.3	0.5568	-99.1	0.9410	-135.6
4.3820	0.6435	177.4	0.1163	-26.2	0.4678	-107.1	0.9436	-142.2
4.9801	0.6335	178.2	0.1138	-32.8	0.3994	-112.1	0.9427	-147.8
5.5784	0.6273	179.1	0.1089	-38.7	0.3560	-116.6	0.9415	-152.5
6.1766	0.6242	-179.8	0.1070	-41.4	0.3206	-122.4	0.9406	-156.4
6.7748	0.6198	-178.8	0.1060	-47.6	0.2898	-129.7	0.9354	-160.0
7.3730	0.6180	-177.3	0.1051	-54.4	0.2513	-134.4	0.9280	-162.8
7.9711	0.6190	-176.0	0.0939	-59.8	0.2243	-137.4	0.9219	-166.1
8.5694	0.6176	-175.3	0.0887	-63.2	0.2070	-141.5	0.9121	-168.7
9.1676	0.6153	-174.3	0.0912	-67.4	0.1881	-146.6	0.8992	-171.1
9.7658	0.6203	-172.7	0.0915	-73.6	0.1763	-151.1	0.8911	-173.3
10.3640	0.6241	-172.0	0.0846	-78.8	0.1600	-156.7	0.8863	-174.8
10.9622	0.6266	-171.5	0.0741	-85.9	0.1419	-161.9	0.8764	-177.1
11.5604	0.6345	-170.5	0.0672	-88.1	0.1320	-163.1	0.8738	-179.6
12.1586	0.6337	-170.3	0.0700	-91.5	0.1279	-166.8	0.8597	177.5
12.9063	0.6377	-169.6	0.0682	-98.6	0.1181	-177.1	0.8548	176.9
13.5045	0.6433	-169.3	0.0558	-107.2	0.0991	177.3	0.8420	174.3
14.1027	0.6428	-168.7	0.0524	-107.0	0.0923	175.9	0.8368	173.7
14.8505	0.6470	-168.1	0.0560	-111.8	0.0918	172.7	0.8103	171.6
14.9252	0.6522	-168.3	0.0524	-111.3	0.0883	172.5	0.8077	171.5
15.0000	0.6591	-168.2	0.0536	-113.0	0.0886	171.7	0.8270	171.4

Table 2.1 S-Parameters of Run 210-1, FINT k

2.4 Extraction of f_T and F_{max}

The most common expression for common-emitter short-circuit current-gain is the ratio of output current to input current with the output terminal shorted. [30] Some of these are:

$$\beta = \frac{y21}{y11} = h21 = -\frac{z21}{z22} = \frac{I_C}{I_B} \tag{2.1}$$

These parameters usually rely on the termination of one port in a short or open and develop ratios of impedance, admittance or transimpedance. At microwave frequencies, the terminations used to provide the shorts and opens are very difficult to implement over broadband. The measurement of active networks in an open or short circuit environment may cause the system to oscillate, making the measurements impossible. The network measurement techniques commonly performed to extract parameters for use in these formulas is inadequate at frequencies above a few MHz. Some other form of network characterization system is needed to make measurements at the higher frequencies.

Scattering parameters are used to characterize the device under test at microwave frequencies. By terminating the input and output ports with the characteristic impedance of the network and measuring the ratio of normalized voltages [31] provide the needed parameters. These parameters are the ratios of reflected waves to incident waves, and transmitted waves to incident waves. The active device is limited and is not as likely to oscillate in this match terminated environment. This allows the collection of these ratios over a large band of frequencies. These S parameters can then be converted into other two-port parameters, i.e. Y, or Z parameters, for analysis [31] by standard transformations.

For this work, S parameter measurements were made on the Hewlett-Packard, HP8510A Automatic Network Analyzer, in common-collector, emitter port 1 and base port 2, configuration. The data is then transformed to the more familiar common-emitter, base port 1, collector port 2 mode. This is done by reversing the order of the ports, i.e. S11 becomes S22, S12 and S21 are swapped and S22 becomes S11. Common-collector S parameters are converted to Y parameters and translated to common-emitter Y parameters by standarized [31] methods. Short-circuit common-emitter current gain, β can be derived from simple formulas. The figure of merit f_T can then be extrapolated from a plot of β vs *frequency*.

2.4.1 Maximum Available Gain

The figure of merit, f_{max} can be determined by extrapolation of a plot of Maximum Available Gain vs *frequency*, M_{AG} of the transistor. That frequency at which the plot of M_{AG} vs *Frequency* crosses the zero-db axis or M_{AG} magnitude is equal to unity from analytical techniques, defines the figure of merit, f_{max}. M_{AG} is measured by conjugately matching the input and output impedances of the transistor. M_{AG} is defined [31] only when the transistor is unconditionally stable. The stability of the transistor is defined by the formula:

$$K = \frac{1 - |S11|^2 - |S22|^2 + |\Delta|^2}{2\,|S12|\,|S21|} \tag{2.2}$$

where

$$|\Delta| = |S11S22 - S12S21| \tag{2.3}$$

When K is equal to 1, the Maximum Stable Gain , M_{SG} is defined as the ratio of the forward transmission coefficient to the reverse transmission coefficient:

$$M_{SG} = \frac{|S21|}{|S12|} \tag{2.4}$$

The Maximum Availiable Gain is defined as:

$$M_{AG} = \frac{|S21|}{|S12|}\left(K - (K^2 - 1)^{½}\right),\ K > 1, B1 > 0 \tag{2.5}$$

where

$$B1 = 1 + |S11|^2 - |S22|^2 - |\Delta|^2 \qquad (2.6)$$

The conditions, $K > 1$ and $B1 > 0$ (or $K > 1$ and $|\Delta| < 1$) are necessary and sufficient conditions for unconditional stability for an active network. It is noted that it is common practice to quote M_{SG} when $K < 1$ and provide additional information regarding the instability of the transistor.

2.4.2 Unilateral Power Gain

Unilateral Power Gain, U_{GAIN} is defined as the gain of the transistor when the reverse transmission coefficient equals zero ($S12 = 0$). The U_{GAIN} is independant of the measurement configuration and can be used to measure gain, and estimate $f_{\max}$ in common-collector or common-emitter or common-base topololgies. The formula for U_{GAIN} [31] is:

$$U_{GAIN} = \frac{1}{1 - |S11|^2} |S21|^2 \frac{1}{1 - |S22|^2} \tag{2.7}$$

The zero-db crossover point of a plot of U_{GAIN} vs *frequency* should be close to the $f_{\max}$ derived from the plot of M_{AG}. The $f_{\max}$ extrapolated from U_{GAIN} plots, are useful. It is appropriate for broad-band measurements and represents the conservative estimate of $f_{\max}$. This is due to the fact [32] that the network is not match terminated and therefore more sensitive to changes in frequency and other parameters. These formulas were implemented and applied to each device bias point using *SIM*, a computer program designed to examine *S* parameters and discussed in Appendix C.

2.4.3 Common-Emitter Short-Circuit Current Gain

The values for f_T were determined by analyzing the data for a dominant pole approximation of *6db/octave*, or a *20db/decade*, β roll off. This method assumes a single dominant pole will produce this slope down to the zero-crossover frequency, f_T. Most devices that were measured, demonstrated this behavior at low frequencies. At higher frequencies, the effects of base-collector parasitics [33] are apparent and the graph deviates from the *20db/decade* slope. Analysis of the $f\beta$ product over a *6db/octave* range in the data, will yield a good analytical estimation of f_T. Using a graphical technique additionally tends to validate this estimate.

2.5 Discussion of Results

The parameters $f_{\max}$ and f_T can be determined by similar methods. For optimistic estimation, determining the zero-crossover frequency, analytically or graphically will specify $f_{\max}$ or f_T. Observation of the *6db/octave* slope shows that $f_{\max}$ can be easily over-estimated, in the FINT devices.

The zero-crossover frequency for the *Unilateral Gain* vs *Frequency* graph or table is usually below $f_{\max}$ derived by the M_{AG} plot. The $f_{\max}$ derived from U_{GAIN} plots are a conservative estimate of the maximum frequency of oscillation.

Comparison of the f_T and $f_{\max}$ values, determined by these methods, to the numbers expected from physical parameters determined previously, show that there exists large deviations. Table 2.2 is an example of the results that show that the extrapolated values of f_T, are far less than the 28 GHz predicted. A typical chart of the performance of these devices at different bias points is illustrated in Figure 2.2.

HIGH FREQUENCY PERFORMANCE OF HBT					
RUN	NAME	DEVICE	BIAS	FT(GHz)	FMAX(GHz)
210-1	k	fint	3v2ma	1.0	1.0
210-1	k	fint	3v5ma	2.5	4.2
210-1	k	fint	3v10ma	3.8	4.7
210-1	k	fint	3v15ma	5.7	5.1
210-1	k	fint	3v20ma	6.4	5.7
210-1	k	fint	3v25ma	7.5	5.7
210-1	k	fint	3v30ma	8.2	6.0
210-1	k	fint	3v35ma	8.8	6.1
210-1	k	fint	3v40ma	9.1	6.1
210-1	k	fint	3v45ma	9.6	6.2
210-1	k	fint	3v50ma	9.8	6.2
210-1	k	fint	3v55ma	10.0	6.2
210-1	k	fint	3v60ma	10.3	6.2
210-1	k	fint	3v65ma	10.4	6.2
210-1	k	fint	3v70ma	10.6	6.2
210-1	k	fint	3v75ma	10.8	6.2
210-1	k	fint	3v80ma	10.9	6.2
210-1	k	fint	3v85ma	10.8	6.2
210-1	k	fint	3v90ma	11.0	6.1
210-1	k	fint	3v95ma	11.0	6.1
210-1	k	fint	3v100ma	11.1	6.0
210-1	k	fint	3v110ma	11.3	6.1

Table 2.2 Data Summary of Run 210-1, FINT K

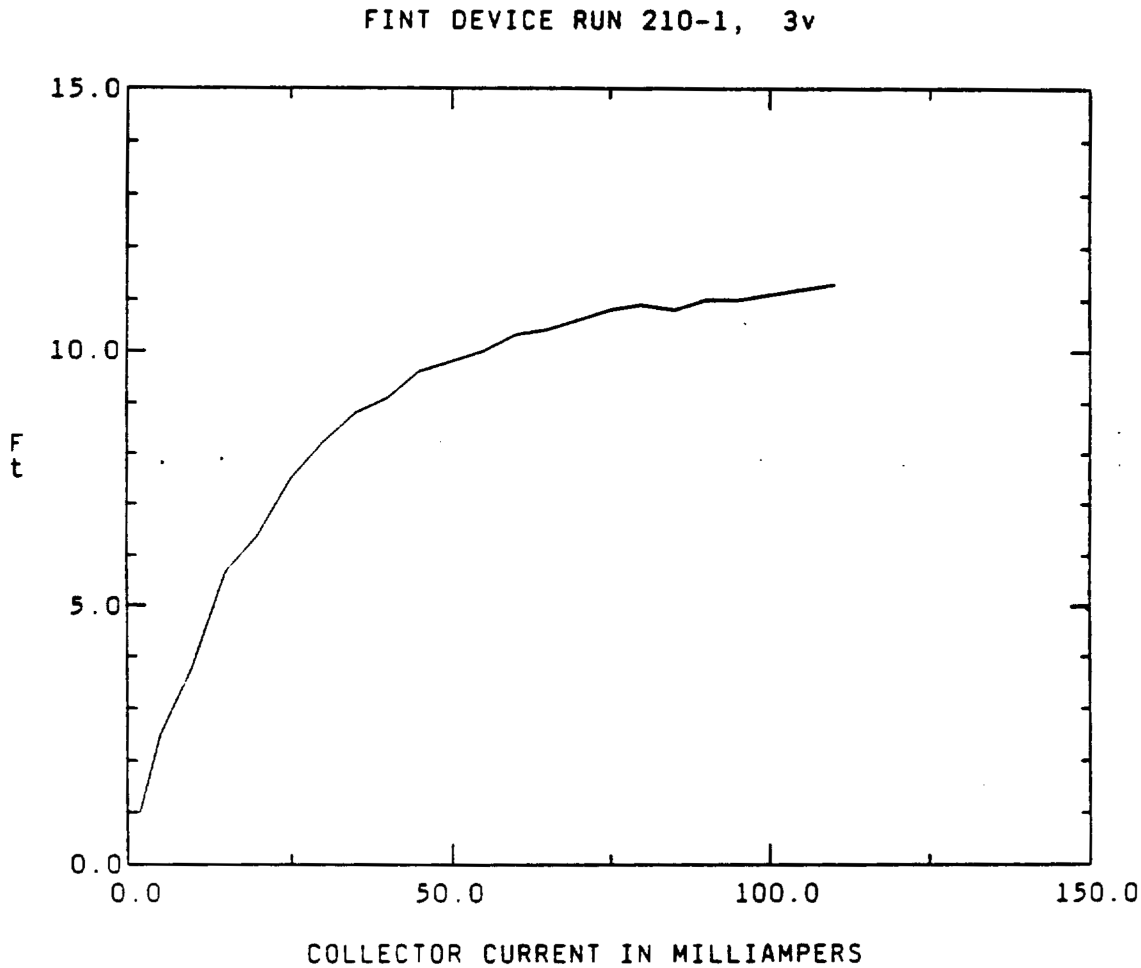

Figure 2.2. Typical FINT Device Performance.

2.6 Graphical Analysis

Valuable insight into possible deviations from theory can be found in a plot of $\frac{1}{2\pi f_t}$ vs $\frac{1}{I_C}$. A sweep of collector currents for a fixed V_{CE} and the respective f_t are plotted, in Figure 2.3. Examining the equation for τ_T shows that it describes an equation for a simple line, i.e.

$$\tau_T = \tau_f + \frac{(C_{je} + C_{jc})}{g_m} + C_{jc}\left[r_e + r_c\right] \tag{2.8}$$

We know that:

$$g_m = \frac{I_C}{V_T} \tag{2.9}$$

Therefore:

$$\tau_T = \tau_f + C_{jc}\left[r_e + r_c\right] + V_T\frac{\left[C_{je} + C_{jc}\right]}{I_E} \tag{2.10}$$

Assuming I_E is equal to I_C, this equation is the formula for a line:

$$y = mx + b \tag{2.11}$$

where:

$$y = \tau_T = \left[2\pi f_T\right]^{-1} \tag{2.12}$$

$$x = \frac{1}{I_E} \tag{2.13}$$

and

$$m = \left[C_{je} + C_{jc} \right] V_T \tag{2.14}$$

$$b = \tau_f + C_{jc} \left[r_e + r_c \right] \tag{2.15}$$

The slope of the plot in the moderate current level area of the Figure 2.3 is:

$$m = \left[C_{je} + C_{jc} \right] V_T = \frac{21.2 - 16.2}{0.04 - 0.02} = 250 \tag{2.16}$$

Thus,

$$C_{je} + C_{jc} = 9.615\, pf . \tag{2.17}$$

From Table 1.2, we have the theoretical values for run 210-1.

$$C_{je} = 5.3\, pf \tag{2.18}$$

$$C_{jc} = 3.29\, pf \tag{2.19}$$

The parasitic capacitances may be assumed to be the difference:

$$C_{pad} = 9.615 – 5.3 – 3.29 \tag{2.20}$$

$$C_{pad} = 1.03\, pf \tag{2.21}$$

The pad capacitors were measured at 1 MHz to be 0.3 pf for this run. There is a net parasitic of 0.73 pf. This extra capacitance may be due to the pad itself or some mechanism in the device, some of which are explained below.

Inspection of Figure 2.3 yields the intercept of the line:

$$b = \tau_f + C_{jc} \, (r_e + r_c) = 10.5\, \text{ps} . \tag{2.22}$$

From Table 1.2, run 210-1 shows a τ_f of 1.89 ps therefore:

$$r_e + r_c = \frac{(10.5 - 1.89)}{C_{jc}} = 2.62\Omega \tag{2.23}$$

This sum, $r_e + r_c$, is 11 times higher than predicted by theory.

Another piece of information that can be found here is r_b. The measured $f_{\max}$ for the K FINT device from run 210-1 was 6.2 GHz. The standard formula for $f_{\max}$:

$$f_{\max} = \left[\frac{f_T}{8\pi C_{jc} r_b} \right]^{½} \tag{2.24}$$

Using the predicted C_{jc} from Table 1.1 and measured f_t of 9.8 GHz:

$$r_b = \frac{f_t}{\left[f_{\max} \right]^2 8\pi C_{jc}} = 3.08\,\Omega\,. \tag{2.25}$$

If the sum of $C_{jc} + C_{pad}$, the parasitic capacitances, are used in a similar manner it would be found:

$$r_e + r_c = 1.99\,\Omega \tag{2.26}$$

and

$$r_b = 2.35\,\Omega \tag{2.27}$$

The circuit values that have been derived by this manner can then be combined with existing theoretical values, providing a tuning range for an optimization procedure. This will be the initial starting point for the optimizer and will enable a valuable solution to be found.

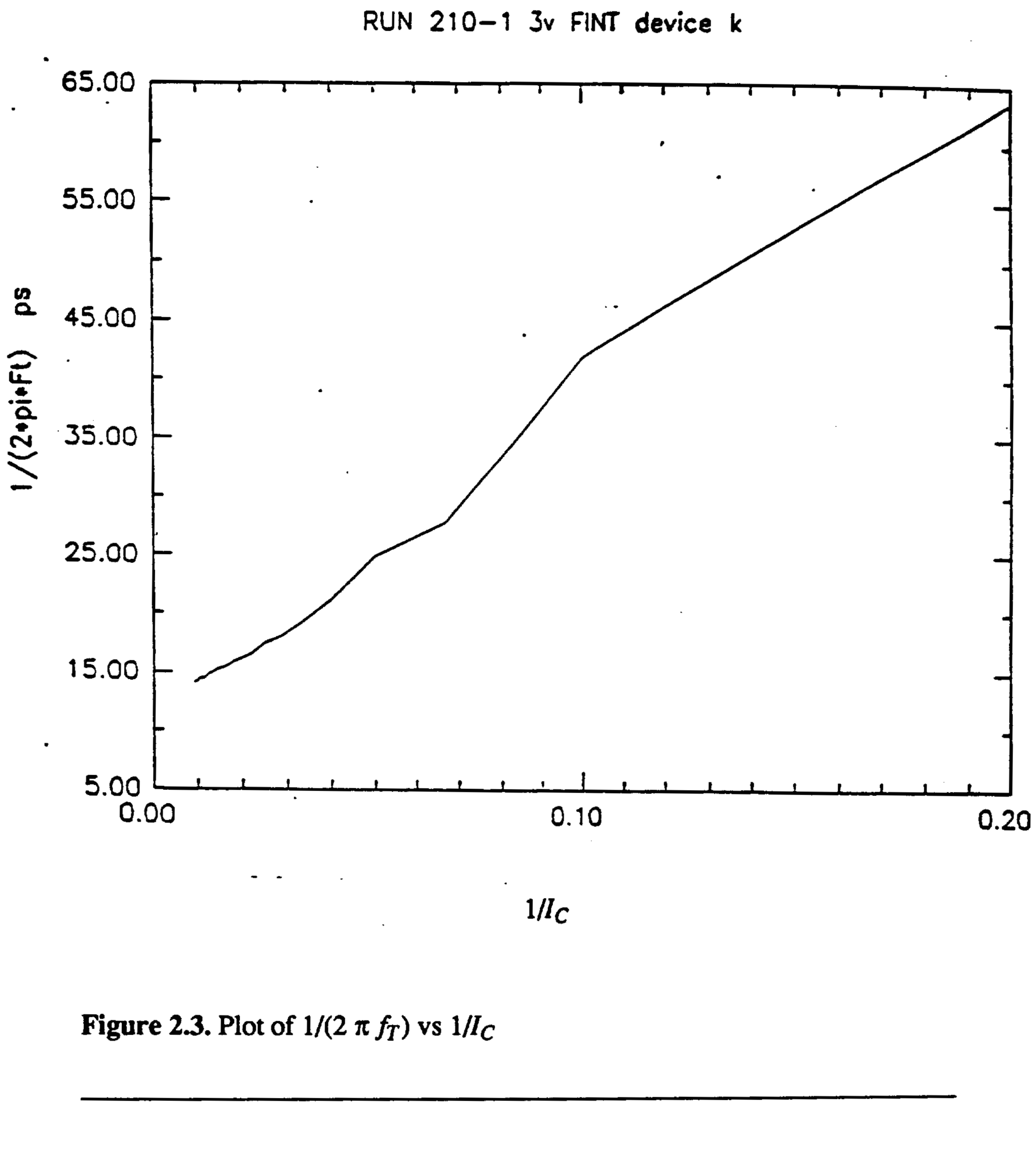

Figure 2.3. Plot of $1/(2\,\pi\, f_T)$ vs $1/I_C$

CHAPTER 3: OPTIMIZATION OF THE EQUIVALENT CIRCUIT MODEL

3.1 Algorithm for Optimization

Even though we have a good physical model and have made adjustments that were derived using the $\frac{1}{2\pi f_t}$ vs $\frac{1}{I_C}$ plot analysis, it is clear that other changes in the model are required.

Optimizers can be a very useful tool. They can automate the very slow process of iteratively selecting new values for an element and testing the resulting circuit response. They mininize an "error function" that is a weighted average of [34] the actual response to the desired response.

A Random Optimizer was first used to select new component values at random within the specified range. It then re-evaluated the error function. When the error function decreased, the optimizer stored the new value and continued to search for a better solution. This method found an adequate result regardless of the initial accuracy of component values.

To find a better solution, the Gradient Optimizer was used. It examines the slope of the error surface and tries to pick element values that will predict a minimum to the error surface. Given good initial values, this Newton type method will converge to a solution very quickly. So, the Random Optimzer was used to find a good initial solution for the Gradient Optimizer.

Summarizing, after chosing a single bias point, the element values were estimated from the physical parameters of the device. Some values were adjusted to meet experimental data or graphical evaluation. From these forms of analysis, possible ranges of these values were estimated.

SUPER-COMPACT generated *S* parameter data files from the derived circuit model file. The use of the optimizer programs built into SUPER-COMPACT was carefully used to improve the match of the estimated circuit file data to measured data and deduce the element values. A plot of this estimated data on a Smith-Chart was useful for comparison to measured data. Good control of the optimization process was maintained by constantly comparing measured data and optimized data on Smith-Charts. For frequencies spanning more than one octave, matching was difficult and the band of interest was broken into several ranges.

3.2 Optimization Method

Matching the data over the measurement band, 45MHz to 15GHz, was difficult. The band was first matched from 45MHz to 2GHz. It was assumed that the resistors and large capacitors have greater influence at the lower frequencies, thus optimizing these parameters in this low-frequency range was performed first. All other elements were held at their estimated values from previous analysis.

This proved to provide a good matching technique in this frequency range. Continuing, elements with little relative variation relative to its magnitude, as the frequency range is increased, were then held at that magnitude. This was done to minimize the number of variables and thus reach a better solution for optimization. From this method of optimization, r_e, r_c, g_m, r_π , and a small fudge factor in g_m: τ_o, were fixed to their optimized values. The optimizer was then swept over the entire range of frequency. The pad capacitances, bond wire inductors, the base spreading network and the C_{je}, C_{jc}, capacitances were then allowed to float over a range of values.

The Random Optimizer was used to estimate a close solution. The gradient method of optimization would deviate from reasonable solutions when it was invoked before the random optimization reached a local solution. The Gradient

Optimizer was used after the random option did not reach a better solution, as determined by the change in the value of the error function supplied by SUPER-COMPACT during execution. However, once a good solution was near, the gradient option found a local solution, quickly.

3.3 Analysis of Optimization

Figure 3.1, is the Smith-Chart representation of $S11$ and $S22$ of the measured data from Run 210-1 FINT device K, biased at 3 volts 50 *ma*. Figure 3.3, contains the $S12$ and $S21$ information in polar form for the same device. After completely optimizing the circuit file, the resulting plot is shown in Figures 3.2 and Figure 3.4. It can be seen from these graphs that the results fit well over a wide band of frequency. The weighting of each S parameter was equal. That is, the data was optimized equally for each S parameter. The magnitude of the error in $S12$, since the parameter $S12$ is usually much smaller than other parameters, can be of the same magnitude as the magnitude of $S12$ and propagate a large error through the result.

The optimized plot of $S11$ surrounds a similar group of points but does not vary as much as the actual data. It is however within the same order of magnitude as the measured data. The $S22$ data matched very well except at the highest frequencies where the effects of the calibration can be seen. The fit of $S12$ and $S21$ plots are very good.

A comparison plot of Gain vs. Frequency for the optimized and measured common-emitter data is shown in Figure 3.5. There was approximately a 20%

variation in the current gain at low frequencies but a better alignment at higher frequencies.

Unilateral Power Gain assumes that S12 is zero. Any error in S12 is not propagated into this calculation and good alignment of the optimized and measured data was obtained. The value for $f_{\max}$, determined from this plot, was considered a most conservative estimate of this figure of merit.

The formula for *MAG* contains $S\,12$ in the denominator. $S\,12$ is usually very small for most devices and is affected greatly by any error that is of the same order of magnitude. Thus the plot of *MAG* does not show fitting characteristics that are as close as those from the U_{GAIN} plot, yet still acceptable.

These plots show that the *HBT* can be modeled by this circuit model. Elements can be estimated from an analysis of the physical parameters of the device, and estimated from analysis of measured data and careful use of a good optimizer. The final version of the circuit file is shown in Figure 3.6. The fully optimized hybrid-π model is illustrated in Figure 3.7. This file lists the final values the optimizer reached for each element.

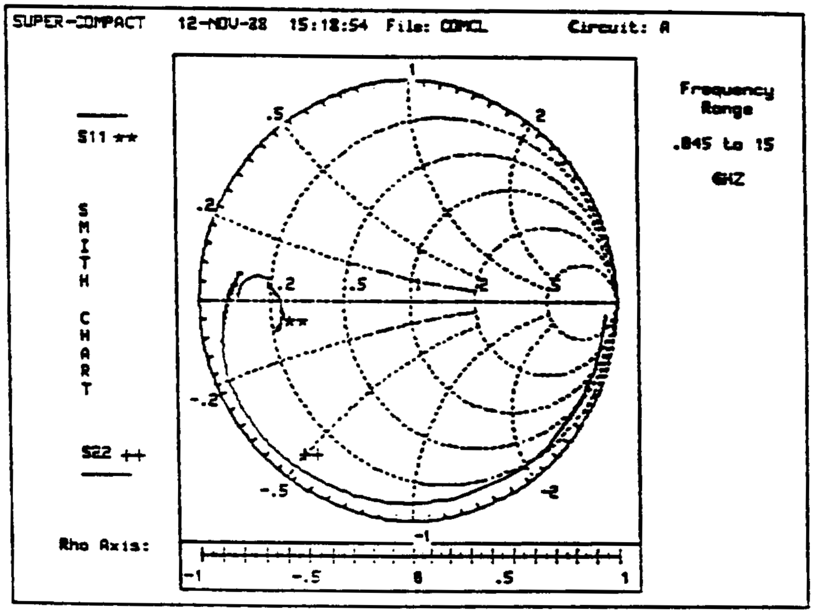

Figure 3.1. The Measured Common-Collector $S11$ and $S22$.

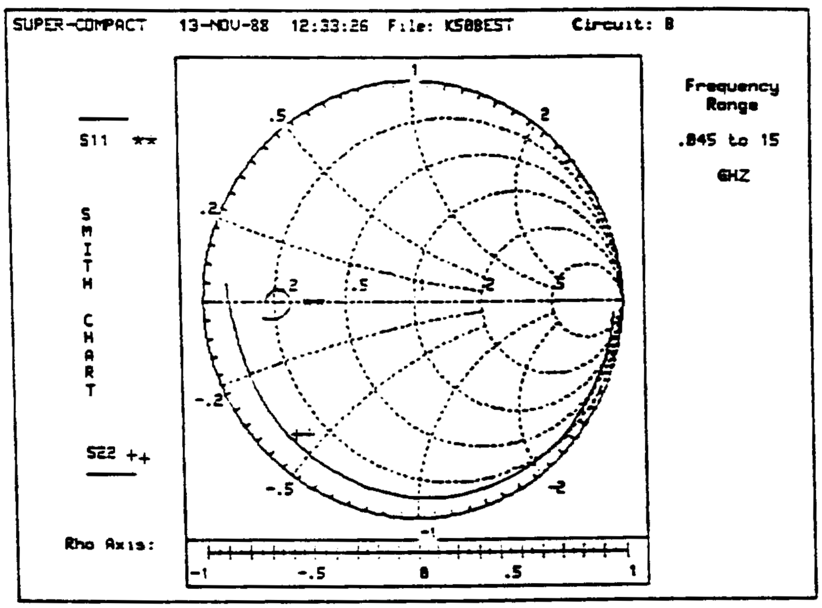

Figure 3.2. The Optimized Circuit Common-Collector $S11$ and $S22$.

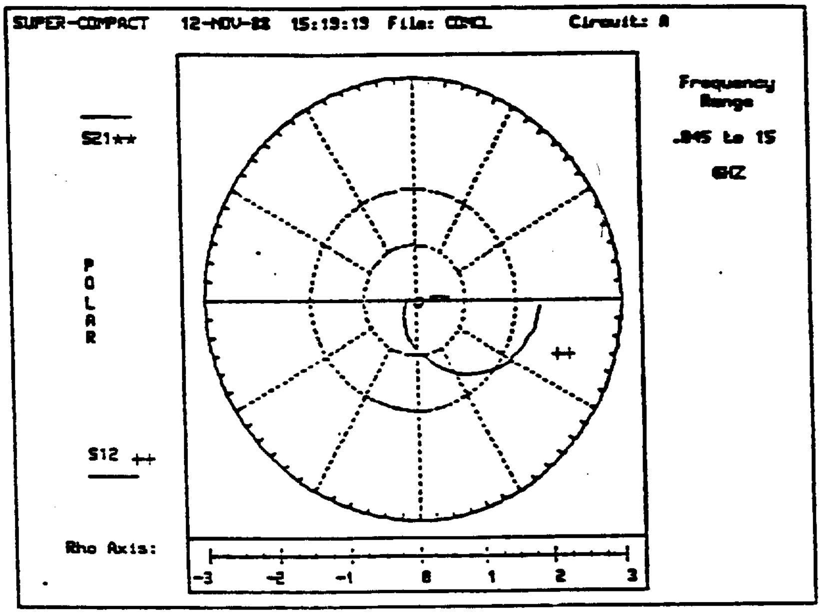

Figure 3.3. The Measured Common-Collector $S\,12$ and $S\,21$.

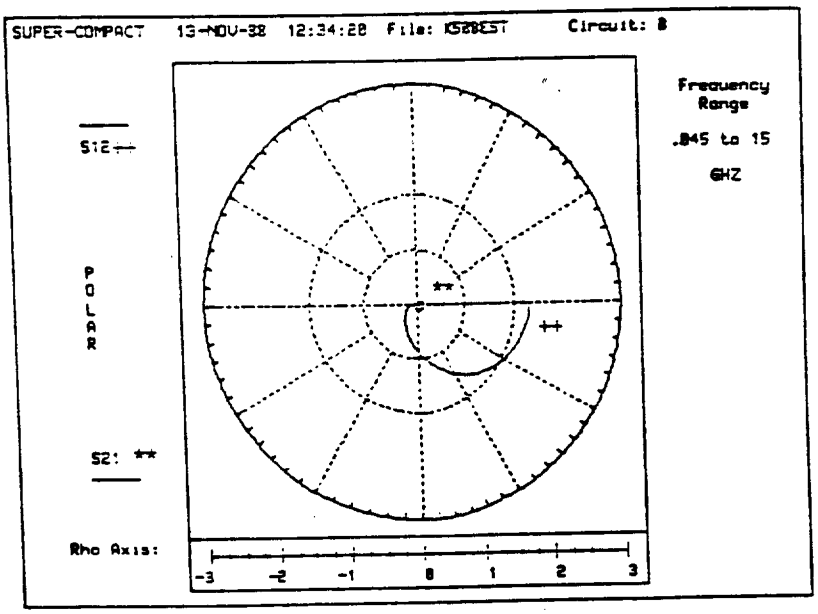

Figure 3.4. The Optimized Circuit Common-Collector $S\,12$ and $S\,21$.

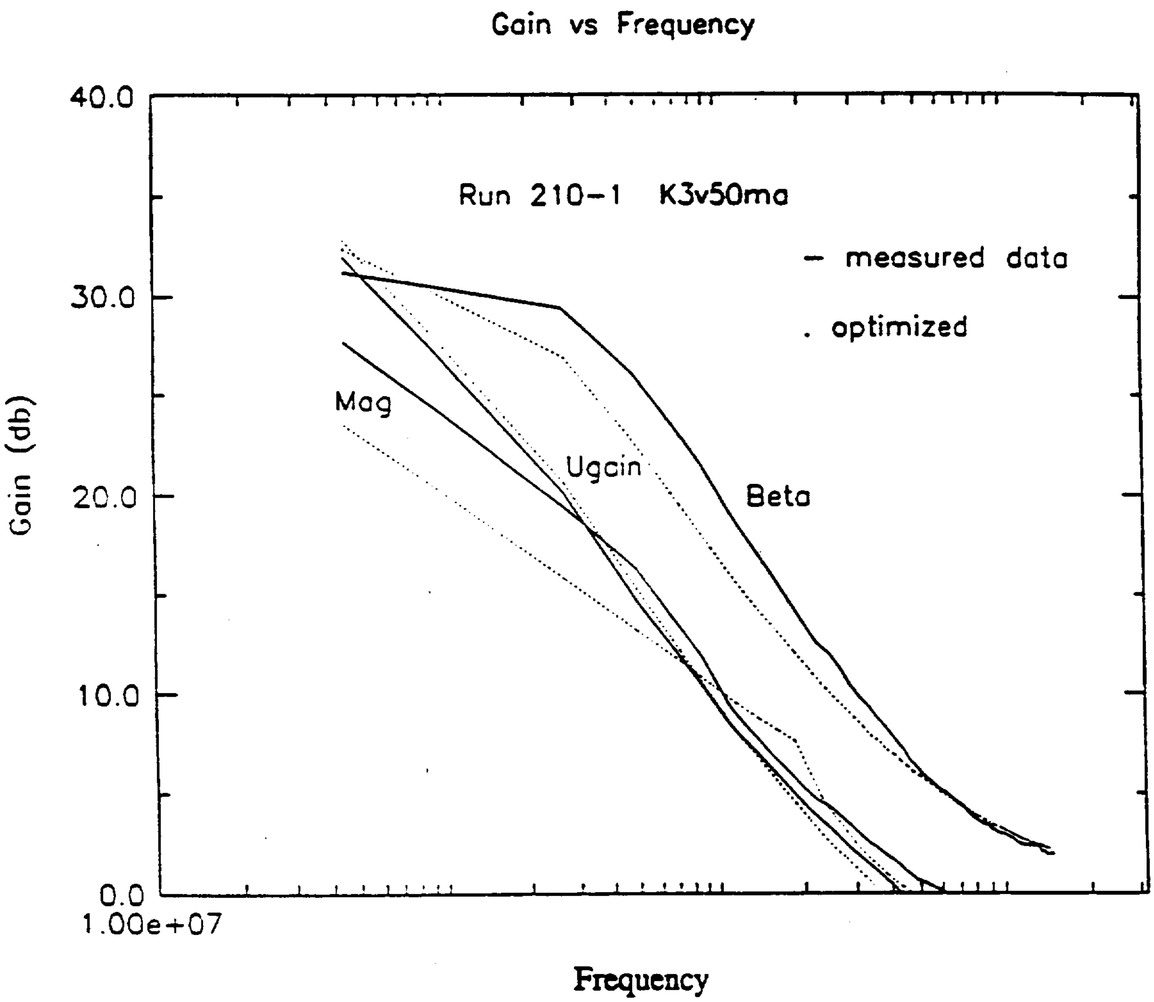

Figure 3.5. Gain vs Frequency plots of Measured and Optimized data.

In the following optimized circuit, g_m was allowed to vary. However, an examiner pointed out that g_m should be constrained to a given value.

```
*   JWM.DAT
*   HBT BIPOLAR TRANSISTOR MODEL
*   COMMON COLLECTOR
*   SIMULATION OF CIRCUIT 2101-1   FINT K 50MA
*
BLK
*
                      LOW VALUE       OPTIMIZED        TOP VALUE

IND 91   1   L   = ? 0.01PH          .09863NH          1NH?
CAP  1   0   C   = ? 0.1PF           1.0263PF          1.5PF?
CAP 11   3   C   = ? 0.01PF          .40414PF          1PF?
CAP 12   3   C   = ? 0.01PF          .29343PF          1PF?
RES  1  11   R   = ? 0.5             8.7165            15?
RES 11  12   R   = ? 0.5             5.8067            9?
RES 12   2   R   = ? 0.5             15.5              15.5?
RES  2   3   R   = 23.301KOH
CAP  2   4   C   = ? 3PF             8.3631PF          12PF?
CAP  2   3   C   = ? .1PF            .35504PF          9PF?
RES  3   0   R   = ? 0.2             2.9886            6?
RES  4   8   R   = ? 0.2             6.2116            10?
CAP  8   0   C   = ? 0.1PF           .74159PF          3PF?
IND 98   8   L   = ? 0.01PH          .05617NH          1NH?

VCG 2 3 4 4  G?1.6614? R1 ?26.59? R2=281.77KOH T=4.4032E-15
B:2POR 98 91
END
```

Figure 3.6. The Final Version of the Test Circuit File.

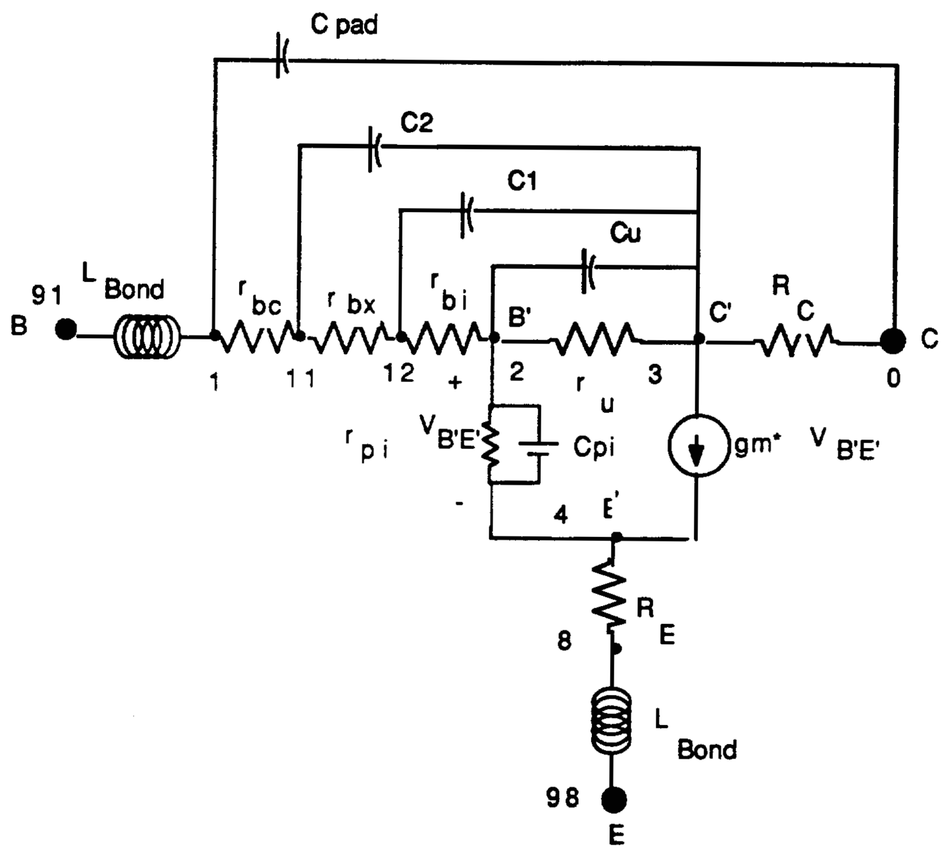

Figure 3.7. The Final Hybrid-π Model, Values in Figure 3.6.

3.4 Analysis of the Resulting Circuit File

From the circuit file created by SUPER-COMPACT shown in Figure 3.6, several items need to be addressed.

It is noticable that there is a change in the optimized value of g_m. The d.c. value of g_m is assumed to be only a factor of I_C and the V_T term. However it appears that there exists a possiblity that the V_T term is affected by a factor of 1.5 to 1.6 instead of the assumed unity. This is possibly due to the effects of the conduction band spike, [11] not being completely suppressed or some other form of material mismatch, surface traps, and other lattice effects.

The value of the base-emitter capacitance C_{jE} seems high. The initial value used and determined by physics of the junction was 5.3 pf. The optimized value is 8.4 pf. This large deviation can be explained by the possiblity that the quality of the junction may not have been ideal. Also the doping levels for this wafer were not varified for this as yet experimental device. Therefore this value for capacitance is possible.

The value for f_T generated by the optimized equivalent circuit taken from Figure 3.7, τ_T with parasitics included becomes:

$$\tau_T = \tau_f + \frac{\left[C_{je} + C_{jc} + C_{pad}\right]}{g_m} + \left[C_{jC} + C_{pad}\right]\left[r_e + r_c\right] \tag{3.1}$$

$$\tau_T = 25.89\text{ps} \tag{3.2}$$

and

$$f_T = 6.1\text{GHz} \tag{3.3}$$

also

$$f_{\max} = 4.8\text{GHz} \tag{3.4}$$

The smaller value of f_T compared to the values determined in the earlier portion of this report is due to the large value of (r_e + r_c) term. The contribution of this term to the degradation of f_t or the increase in τ_f is 12.9 ps. This component was not separated into r_e and r_c in this work. However it is believed from d.c. measurements on a curve tracer from previous devices that the emitter resistance is the most likely problem. A FINT device with such a large area should have this resistance sum closer to 0.1 ohm.

Given what is known about the wafer doping levels, it does not appear that τ_f is the major problem. The process for isolation of the discrete devices seems to be the culprit. The emitter-base junction is the area that needs attention.

The large capacitors in the junctions are functions of the active area. Smaller devices should yield higher performance by simply smaller areas. These smaller devices were not availiable for this analysis on a consistant basis.

The d.c. current gain of this device can be determined by the $g_m * r_\pi$ product. From the circuit file this value is 44 which is very close to the value determined at d.c. This is a good check on the performance of the optimization. The current source shows slightly non-ideal characteristics, as shown by g_m and the small time constant needed. The R_{out} resistor can be ignored from the model. The value for τ_o used in the current source is merely a factor used to account for any extra phase shift in the base network not modeled in the circuit. It is very small and could also be ignored.

The Early effect resistor r_u is much smaller than the 100k ohm value normally assumed in this model. The junction is probably leaky. But the RC time constant of the base-collector junction is still very long (50ps) compared to others in the circuit. This parameter could also be ignored.

The distributed base network has values that seem to be large for this device. This is possibly due to base contacts and the large spacing between fingers.

The bond wire inductors were introduced into the model to account for the deviation in the length of the wire bonds used to launch the signal to this device and those used on the calibration substrate. The lengths of the bond wires are clearly not completely calibrated out of the measurements.

The parasitic bond pad capacitances are much higher than calculated or measured at 1MHz. The values for the capacitances initially were determined by measuring metal disks, simulating bond pads, on an HBT wafer. The value determined may be good at 1MHz but may not be valid at the microwave frequencies. The dielectric is known to have an ε_r that is a function of thickness. It may also be highly frequency dependent.

A table comparing the circuit elements for the three stages of the project is shown in Table 3.1.

COMPARISON OF PARAMETERS BY STAGE			
Element	Initial	Tuned	Optimized
r_{bx}	6.67		5.8
r_{bi}	10		15.5
r_{bc}	326		8.72
r_b	342	2.35	30.0
r_e	0.12		6.21
r_c	0.12		2.98
$r_e + r_c$	0.24	2.62	9.19
g_m	1.93	1.93	1.66
$C_{jc(pf)}$	3.29	3.29	0.355
$C_{je(pf)}$	5.30	5.30	8.36
$C_{pad(pf)}$	0.3	1.03	1.03

Table 3.1 The Lumped Element Values by Stage

CHAPTER 4: SUGGESTIONS FOR IMPROVING DEVICE PERFORMANCE

The size of the devices and the spacing of the fingers must be reduced to fully exploit the potential the HBT has to offer. Smaller active areas and smaller line widths can produce larger f_T and $f_{\max}$ values.

Each wafer should be analyzed for doping profile before any processing is performed. If this step is avoided, a systematic error can propagate throughout the process.

The base-emitter junction needs further analysis as this junction clearly limits device performance. Hanging metal, alignment problems and undercut can cause hot-spots to develop and limit the device to lower than ideal current levels and voltages. Maximum performance of this device is restricted to the quality of this junction due to its contribution to f_T. The height of the wafer itself may limit the device as current levels increase and thermal effects of the bulk substrate become apparent. This wafer should be thinned to help aid in the dissipation of heat. The emitter and collector resistances should be minimized to improve the performance of the device.

The quality of the nitride used as lift-off and cap material as well as the dielectric under the pads must also be improved. The dielectric constant of this material must be accurately determined over the frequency range of interest and must not be a function of layer thickness.

If the collector-down discrete process is to be continued, the ground plane of the bond pads should be removed as far from the metal pad as possible. This will lower the parasitic capacitance. Two microns or more, and a good dielectric under the pads would isolate the effects of the pad capacitance and increase f_T.

Finally, the semi-insulating property of intrinsic GaAs should be exploited by the development of a collector-up planer process. This would reduce pad capacitances.

CHAPTER 5: CONCLUSIONS

It has been shown that the HBT was characterized using standard techniques for any bipolar transistor. The equivalent circuit model parameters were estimated from a first order physics model. Graphical techniques were used to estimate the element values from collected device data. Prudent optimization techniques were employed to provide an equivalent circuit model that can be explained from physical structures. The hybrid-π model was altered to show good device behavior to 15 GHz.

Figures of merit, (f_T and $f_{\max}$) were extracted from the measured devices and showed problems limiting the speed of the current HBT process. The device could operate at high frequencies if changes were made in the mask and the process optimized to reduce parasitic resistance.

A computer program was written to extract figures of merit from data in a single pass. This is an improvement over previous techniques requiring several passes by the computer.

REFERENCES

References

1. B. L. Sharma and R. K. Purohit, *Semiconductor Heterojunctions,* Pergamon Press, Elmsford, New York, 1974.

2. H. Kroemer, ''Theory of a Wide-Gap Emitter for Transistors,'' *Proc. IRE*, vol. 45 no. 11, pp. 1535-1537, 1957.

3. H. Kroemer, ''Heterostructure Bipolar Transistors and Integrated Circuits,'' *Proc. IRE*, vol. 70 no. 1, pp. 13-25, 1982.

4. H. Kroemer, ''Heterostructure Bipolar Transistors: What Should We Build?,'' *J. Vac.Sci.Technol.*, vol. B1 no. 2, pp. 126-130, 1983a.

5. M. H. White and M. O. Thurston, ''Characterization of Microwave Transistors,'' *Solid-State Electronics*, vol. 13, pp. 523-542, 1970.

6. Harry F. Cooke, ''Microwave Transistors: Theory and Design,'' *Proceedings of the IEEE*, vol. 59 no. 8, pp. 1163-1181, August 1971.

7. C. W. Clawson, ''A Literature Survey on Heterojunction Bipolar Transistors, Part I: Device Structure and Performance,'' *Tektronix Solid State*

Laboratory Technical Report NO. SSRL-86-1, November 7, 1986.

8. P. M. Asbeck, D. L. Miller, W. C. Petersen, and C. G. Kirkpatrick, "GaAs GaAlAs Heterojunction Bipolar Transistors With Cutoff Frequencies Above 10 GHz," *IEEE Electron Device Letters*, vol. EDL-3, no. 12, pp. 366-368.

9. C. W. Clawson, "The AlGaAs/GaAs Heterojunction Bipolar Transistor: Comparative Technology Assessment," *Tektronix Solid State Laboratory Technical Report NO. SSRL-87-3*, Febuary 24, 1987.

10. R. S. Muller and T. I. Kamins, *Device Electronics for Integrated Circuits,* p. 282, Wiley, 1986.

11. C. W. Clawson, "A Literature Survey on Heterojunction Bipolar Transistors, Part II: Device Physics and Modeling," *Tektronix Solid State Laboratory Technical Report NO. SSRL-86-2*, p. 6, November 7, 1986.

12. S. M. Sze, *Physics of Semiconductor Devices, 2nd Edition,* Wiley, 1981.

13. A. B. Phillips, *Transistor Engineering,* McGraw-Hill, 1962.

14. I. Getreu, *Modeling the Bipolar Transistor,* Tektronix, Beaverton, Oregon, 1976.

15. M.B. Das, ''High-Frequency Performance Limitations of Millimeter-Wave Heterojunction Bipolar Transistors,'' *IEEE Trans.Electron Devices*, vol. 35(5), pp. 604-614, 1988.

16. T.H. Ning and D. D. Tang, ''Base Resistance,'' *IEEE Trans. Electron Devices*, vol. ED-31, pp. 409-412.

17. G. K. Reeves and H.B. Harrison, ''Obtaining the Specific Contact Resistance from Transmission Line Model Measurements,'' *IEEE Electron Device Letters*, vol. EDL-3(5), pp. 111-113, 1982.

18. C. W. Clawson, ''Frequency Response of the HBT,'' *Tektronix Solid State Laboratory Technical Report*, July 20, 1988.

19. H. H. Berger, ''Models For Contacts To Planer Devices,'' *Solid-State Electron*, vol. 15, pp. 145-158, 1982.

20. *HP 8510A Operating and Programming Manual,* Hewlett Packard, Santa Rosa, California, 1987.

21. Glen Elmore, ''De-Embed Device Data With a Network Analyzer,'' *Microwaves & RF*, pp. 144-149, November 1985.

22. Jim Fitzpatrick, ''Error Models for Systems Measurement,'' *Microwave Journal*, pp. 63-66, May 1978.

23. David Brubaker, ''Measure S-Parameters with the TSD Technique,'' *Microwaves & RF*, pp. 97-102, November 1985.

24. Jim Mattern, ''De-embedding S-parameter Measurements Using TSD Technique,'' *Air Force Office of Scientific Research Summer Research Program*, Air Force Office of Scientific Research, Washington, DC, 1987. USAF-UES Summer Research Program, Wright-Patterson AFB

25. Doug Rytting, ''An Analysis of Vector Measurement Accuracy Enhancement Techniques,'' *Rf & Microwave Measurement Symposium and Exhibition*, Hewlett Packard, 1987.

26. Doug Rytting, ''Appendix to Analysis of Vector Measurement Accuracy Enhancement,'' *RF & Microwave Measurement Symposium and Exhibition*, Hewlett Packard, 1987.

27. Doug Rytting, ''Advances in Microwave Error Correction Techniques,'' *RF & Microwave Measurement Symposium and Exhibition*, Hewlett Packard, 1987.

28. Compact Software Inc, *SUPER_COMPACT*, Compact Software, INC, Palo Alto, CA. computer programs

29. K.C. Gupta, Ramesh Garg, and Rakesh Chadha, *Computer Aided Design of Microwave Circuits,* Artech House, Inc, Dedham, Massachusetts, 1981.

30. J. A. Nilsson, *Electric Circuits,* Addison-Wesley, 1983. chapter 20

31. G. Gonzalez, *Microwave Transistor Amplifiers, Analysis and Design,* Prentice-Hall, 1984. pp 8-12

32. G. O. Ladd and D. L. Feucht, "Performance Potential of Heterojunction Transistors," *IEEE Electron Devices*, vol. ED-17, pp. 413-420, 1970.

33. P. J. van Wijen and L. C. Smith, "High Frequency Characterization of Small Geometry Transistors," *IEEE 1988 Bipolar Circuits and Technology Meeting*, 1988. paper 5.1

34. Daren McClearon, "Using CAE to Model A 2 to 20 GHz Amplifier," *RF & Microwave Measurement Symposium and Exhibition*, Hewlett Packard, 1988.

APPENDIX A: Notation

The symbols and notation found in this work are shown below:

A_E	Emitter area (μm^2)
A_C	Collector area (μm^2)
β	Current gain
c_π	emitter junction capacitance and diffusion capacitance
c_μ	collector junction and Early effect capacitance
d_C	Width of the collector-base space charge region (calculated)
d_E	Width of the emitter-base space charge region (calculated)
D_{pE}	Diffusivity of holes in the emitter (calculated)
D_{nB}	Diffusivity of electrons in the base (calculated)
ΔE_g	Energy gap offset between AlGaAs and GaAs (eV)
ε_s	Dielectric constant of GaAs (F/cm)
γ	Emitter injection efficiency (calculated)
g_m	transconductance of the dependant current source
I_C	Collector current (mA)
I_E	Emitter current (mA)
k	Boltzmann constant (JK^{-1})

L_e	Emitter stripe length (μm)
L_T	Transfer length of base contact (calculated μm)
μ_{pE}	Mobility of holes in the emitter $200(cm^2V^{-1}s^{-1})$
μ_{nB}	Mobility of electrons in the base $2000(cm^2V^{-1}s^{-1})$
N_{dE}	Donor density in the emitter (cm^{-3})
N_{aB}	Acceptor density in the base (cm^{-3})
N_{dC}	Donor density in the collector (cm^{-3})
n_i	Intrinsic carrier density of GaAs (2.25×10^6)
q	Magnitude of electron charge (C)
ρ_{E1}	Resistivity of the GaAs emitter (Ωcm)
ρ_{E2}	Resistivity of the AlGaAs emitter (Ωcm)
ρ_{IB}	Sheet Resistance of the intrinsic base ($\Omega/\square$)
ρ_{XB}	Sheet resistance of the extrinsic base ($\Omega/\square$)
ρ_C	Resistivity of the collector (Ωcm)
ρ_{sk}	Sheet resistance under the base contact (calculated $\Omega/\square$)
ρ_{cn}	*n*-type specific contact resistivity (Ωcm^2)
ρ_{cp}	*p*-type specific contact resistivity (Ωcm^2)
r_b	base resistance
r_c	collector series resistance

r_e emitter series resistance

r_μ early effect resistance

r_π dynamic base resistance

S_b Base stripe width (μm)

S_e Emitter stripe width (μm)

T Absolute temperature (K)

v_s Saturated electron velocity in GaAs (cm/s)

V_T Thermal voltage, kT/q

V_A Early voltage (V)

V_{BE} Base-emitter bias voltage (V)

V_{CE} Collector-emitter bias voltage (V)

W_B Base width (μm)

W_C n^- Collector width (μm)

W_E Total emitter width, $W_{E0}+W_{E1}+W_{E2}$

W_{E0} Width of emitter cap (μm)

W_{E1} Width of GaAs emitter (μm)

W_{E2} Width of AlGaAs emitter quasi-neutral region (μm)

X_{eb} Emitter-base spacing (μm)

APPENDIX B: FINT Performance Charts and Graphs

Device results are collected in this appendix.

HIGH FREQUENCY PERFORMANCE OF HBT					
RUN	NAME	DEVICE	BIAS	FT	FMAX
136-1	4l	4x2	3v1ma	1	
136-1	4l	4x2	3v2ma	1	
136-1	4r	4x10	3v15ma	5.6	
136-1	4r	4x10	3v25ma	6.1	
136-1	4r	4x10	3v35ma	5.5	
136-1	5l	4x2	3v2ma	1.3	9.9
136-1	5l	4x2	3v4ma	1.5	9.8
136-1	5l	4x2	3v8ma	1	9.4
136-1	5r	4x10	3v15ma	5.6	
136-1	5r	4x10	3v25ma	6.3	
136-1	5r	4x10	3v35ma	4.5	
136-1	5r	4x10	5v35ma	2	
136-1	7l	4x2	3v1ma		
136-1	7l	4x2	3v2ma	1.0	
136-1	7r	4x10	3v4ma	6.0	

Table B.1.1. Data Summary of Run 136-1, 4X10

HIGH FREQUENCY PERFORMANCE OF HBT					
RUN	NAME	DEVICE	BIAS	FT	FMAX
136-1	s1	fint	3v5ma	4	
136-1	s1	fint	3v10ma	6.6	5.0
136-1	s1	fint	3v15ma	7.5	5.0
136-1	s1	fint	3v25ma	8.7	5.5
136-1	s1	fint	3v30ma	9.5	6.0
136-1	s1	fint	3v50ma	10.5	5.75
136-1	s1	fint	4v5ma	4.0	
136-1	s1	fint	4v10ma	6.8	5.25
136-1	s1	fint	4v15ma	8.0	5.5
136-1	s1	fint	4v25ma	9.2	6.0
136-1	s1	fint	4v50ma	10.5	6.0
136-1	s1	fint	5v5ma	4	
136-1	s1	fint	5v10ma	6.0	5.25
136-1	s1	fint	5v15ma	7.5	6.5
136-1	s1	fint	5v25ma	8.7	6.0
136-1	s1	fint	5v30ma	9.0	6.0
136-1	s1	fint	5v50ma	10.2	6.0

Table B.1.2. Data Summary of Run 136-1, FINT

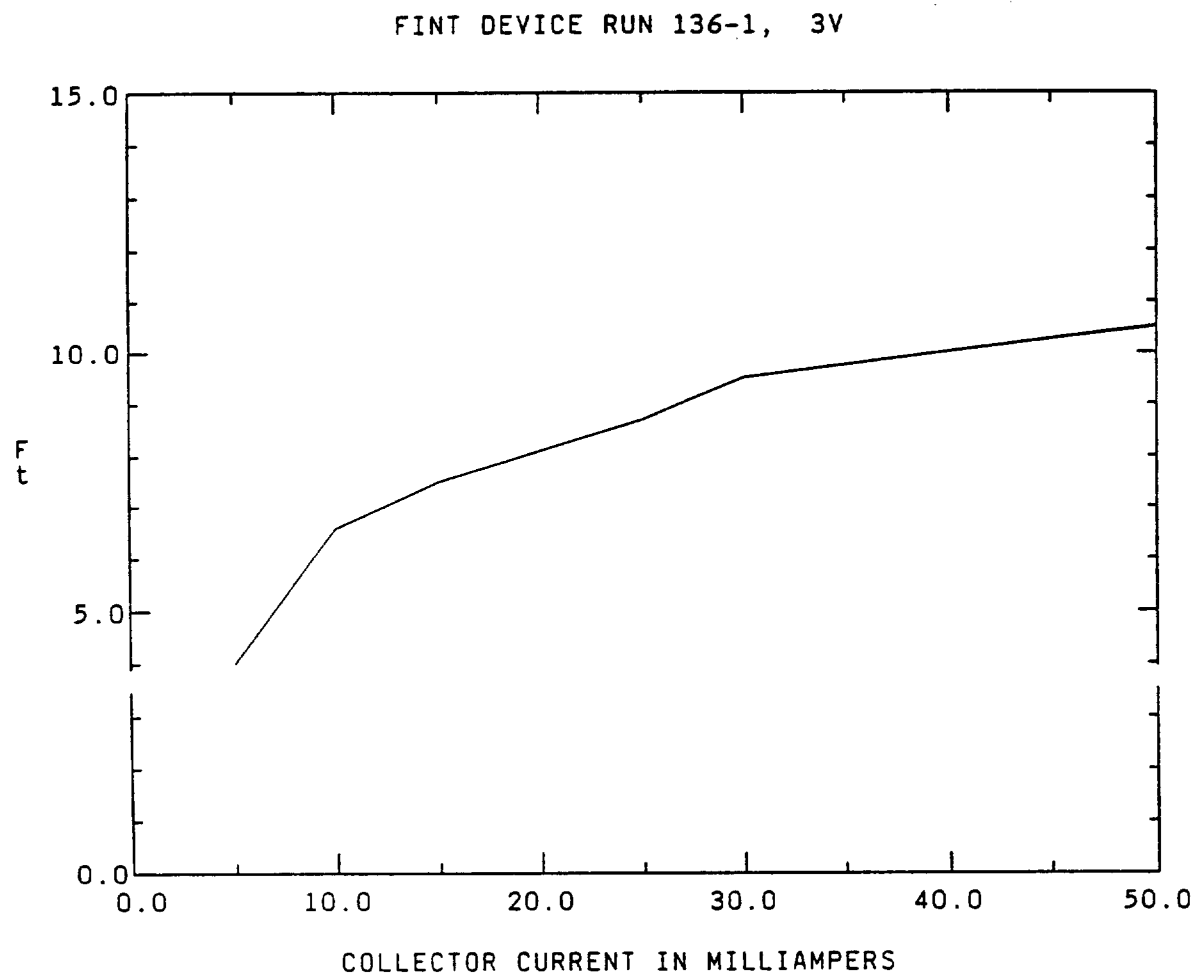

Figure B.1.2. f_T vs Collector Current, 3V

HIGH FREQUENCY PERFORMANCE OF HBT					
RUN	NAME	DEVICE	BIAS	FT	FMAX
136-2	a1	fint	2v5ma		
136-2	a1	fint	2v10ma		
136-2	a1	fint	2v20ma	3.5	2.5
136-2	a1	fint	2v30ma	3.7	2.7
136-2	a1	fint	2v50ma	3	
136-2	a1	fint	3v2ma		
136-2	a1	fint	3v5ma		
136-2	a1	fint	3v10ma		
136-2	a1	fint	3v15ma	3.4	2.5
136-2	a1	fint	3v20ma	3.8	2.8
136-2	a1	fint	3v30ma	4.6	3.1
136-2	a1	fint	3v50ma	5.5	3.25
136-2	a1	fint	3v75ma	5.4	3.25
136-2	a1	fint	3v100ma	5.8	3.25
136-2	a1	fint	3v125ma	6.0	3.25
136-2	a1	fint	3v150ma	6.2	3.25
136-2	a1	fint	5v15ma	3.6	3.00
136-2	a1	fint	5v30ma	5.0	3.5
136-2	a1	fint	5v50ma	6.1	3.75
136-2	a1	fint	5v75ma	6.6	3.0
136-2	a1	fint	5v100ma	7.0	4.0
136-2	a1	fint	5v125ma	7.0	4.0
136-2	a1	fint	5v150ma	6.0	3.75
136-2	a4	fint	2v10ma	2.4	1.75
136-2	a4	fint	2v20ma	3.3	2.0
136-2	a4	fint	3v10ma	2.5	2.0
136-2	a4	fint	3v20ma		
136-2	a4	fint	3v30ma		
136-2	a4	fint	3v50ma	2.8	

Table B.1.3. Data Summary of Run 136-2, FINT

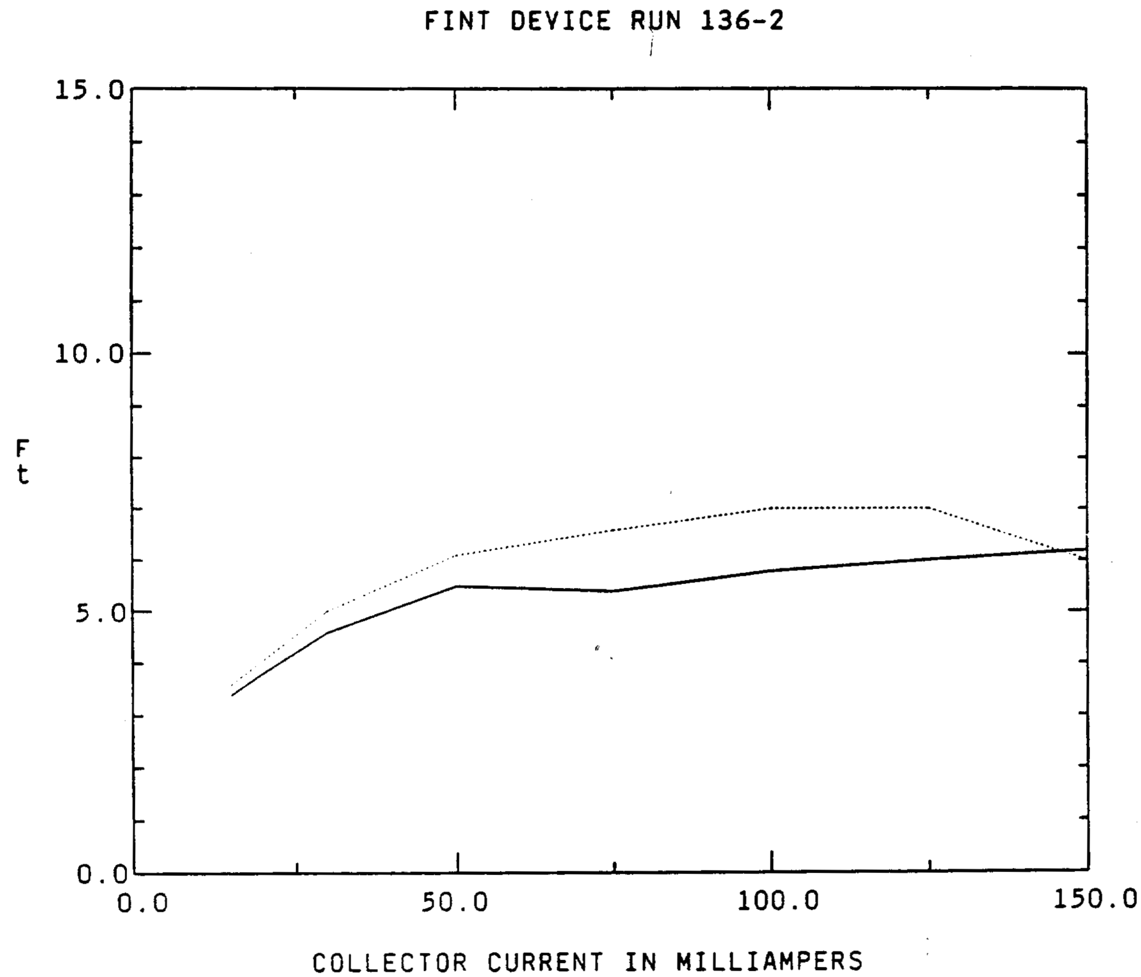

Figure B.1.3. f_T vs Collector Current, 3V, 4V

HIGH FREQUENCY PERFORMANCE OF HBT					
RUN	NAME	DEVICE	BIAS	FT	FMAX
163-1	1a	fint	3v5ma	3.0	8.0
163-1	1a	fint	3v10ma	4.3	8.0
163-1	1a	fint	3v20ma	6.4	8.0
163-1	1a	fint	3v30ma	6.4	8.0
163-1	1a	fint	3v50ma	7.0	8.0
163-1	1a	fint	3v75ma	6.7	8.0
163-1	1a	fint	3v100ma	7.5	7.5
163-1	1a	fint	3v125ma	7.6	7.0
163-1	1a	fint	3v150ma	7.0	6.5
163-1	1a	fint	3v175ma	7.5	6.5
163-1	1a	fint	3v200ma	7.6	5.5
163-1	1a	fint	5v5ma	2.9	8.5
163-1	1a	fint	5v10ma	4.5	8.5
163-1	1a	fint	5v20ma	6.5	8.5
163-1	1a	fint	5v30ma	6.8	8.5
163-1	1a	fint	5v50ma	7.0	8.0
163-1	1a	fint	5v75ma	7.4	7.0
163-1	1a	fint	5v100ma	7.5	6.0
163-1	1a	fint	5v125ma	7.0	5.5
163-1	f2	fint	3v10ma	5.0	
163-1	f2	fint	3v25ma	8.0	
163-1	f2	fint	3v35ma	8.4	
163-1	f2	fint	3v50ma	9.4	7.5
163-1	f4	fint	3v10ma	5.7	
163-1	f4	fint	3v25ma	8.0	
163-1	f4	fint	3v35ma	8.4	
163-1	f4	fint	3v35ma	8.4	

Table B.2.1. Data Summary of Run 163-1, FINT

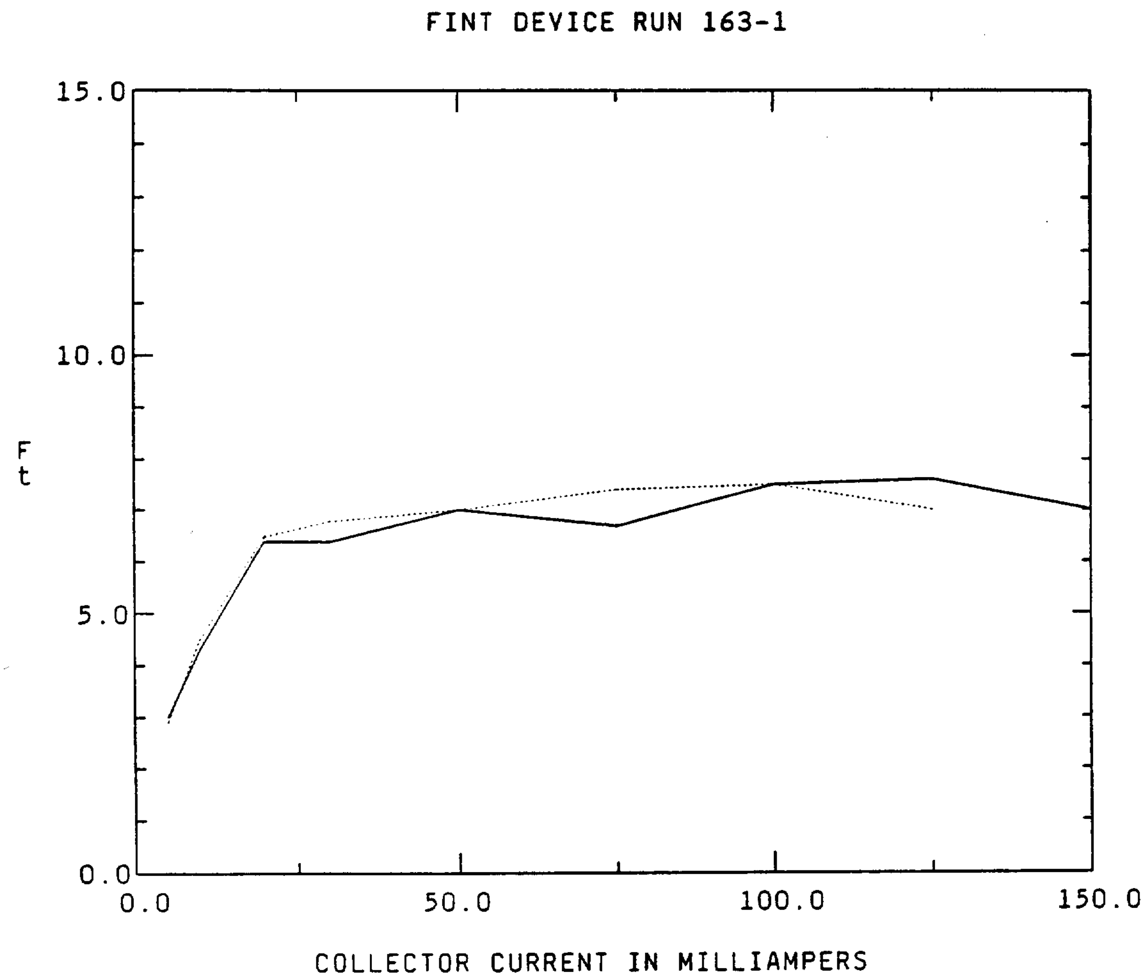

Figure B.2.1. f_T vs Collector Current, 3V, 4V

HIGH FREQUENCY PERFORMANCE OF HBT					
RUN	NAME	DEVICE	BIAS	FT	FMAX
186-2	h	fint	3v2ma	1.0	8.2
186-2	h	fint	3v5ma	2.4	7.8
186-2	h	fint	3v15ma	6.2	8.1
186-2	h	fint	3v30ma	9.0	8.4
186-2	h	fint	3v50ma	10.6	9.0
186-2	h	fint	3v70ma	12.0	9.0
186-2	h	fint	3v100ma	12.3	9.0
186-2	h	fint	3v110ma	13.0	8.8
186-2	h	fint	3v120ma	10.6	8.4
186-2	h	fint	3v130ma	10.5	8.5
186-2	h	fint	3v140ma	10.3	8.5
186-2	h	fint	3v150ma	10.2	8.5
186-2	h	fint	4v2ma	1.0	9.0
186-2	h	fint	4v5ma	2.5	8.2
186-2	h	fint	4v15ma	6.6	8.6
186-2	h	fint	4v30ma	9.0	9.0
186-2	h	fint	4v40ma	9.3	9.6
186-2	h	fint	4v50ma	10.0	9.5
186-2	h	fint	4v60ma	10.7	9.2
186-2	h	fint	4v90ma	11.0	9.5
186-2	h	fint	4v100ma	11.0	9.3
186-2	h	fint	4v110ma	10.5	9.0
186-2	h	fint	4v120ma	9.8	9.0
186-2	h	fint	4v130ma	9.6	9.0
186-2	h	fint	4v140ma	9.6	8.5
186-2	h	fint	4v150ma	9.2	8.5

Table B.3.1. Data Summary of Run 186-2, FINT 3-4V

HIGH FREQUENCY PERFORMANCE OF HBT					
RUN	NAME	DEVICE	BIAS	FT	FMAX
186-2	h	fint	5v2ma	1.0	1.0
186-2	h	fint	5v5ma	2.5	8.5
186-2	h	fint	5v10ma	3.4	8.7
186-2	h	fint	5v15ma	7.0	8.9
186-2	h	fint	5v30ma	7.9	9.4
186-2	h	fint	5v50ma	8.8	9.6
186-2	h	fint	5v90ma	8.6	9.1
186-2	h	fint	5v100ma	8.3	9.0
186-2	h	fint	5v110ma	7.8	8.6

Table B.3.2. Data Summary of Run 186-2, FINT 5V

HIGH FREQUENCY PERFORMANCE OF HBT					
RUN	NAME	DEVICE	BIAS	FT	FMAX
186-2	i	fint	3v2ma	1.5	9.0
186-2	i	fint	3v5ma	3.0	8.4
186-2	i	fint	3v10ma	5.2	8.6
186-2	i	fint	3v15ma	6.9	8.9
186-2	i	fint	3v20ma	9.1	8.5
186-2	i	fint	3v30ma	9.7	9.4
186-2	i	fint	3v40ma	10.5	9.4
186-2	i	fint	4v5ma	2.8	9.1
186-2	i	fint	4v30ma	9.8	10.1
186-2	i	fint	5v2ma	1.2	10.6
186-2	i	fint	5v5ma	3.0	10.1
186-2	i	fint	5v10ma	5.0	10.1
186-2	i	fint	5v15ma	7.0	10.1
186-2	i	fint	5v40ma	10.0	10.3
186-2	i	fint	7v5ma	3.0	10.6
186-2	i	fint	7v10ma	5.0	10.3
186-2	i	fint	7v20ma	8.0	10.6

Table B.3.3. Data Summary of Run 186-2, FINT i

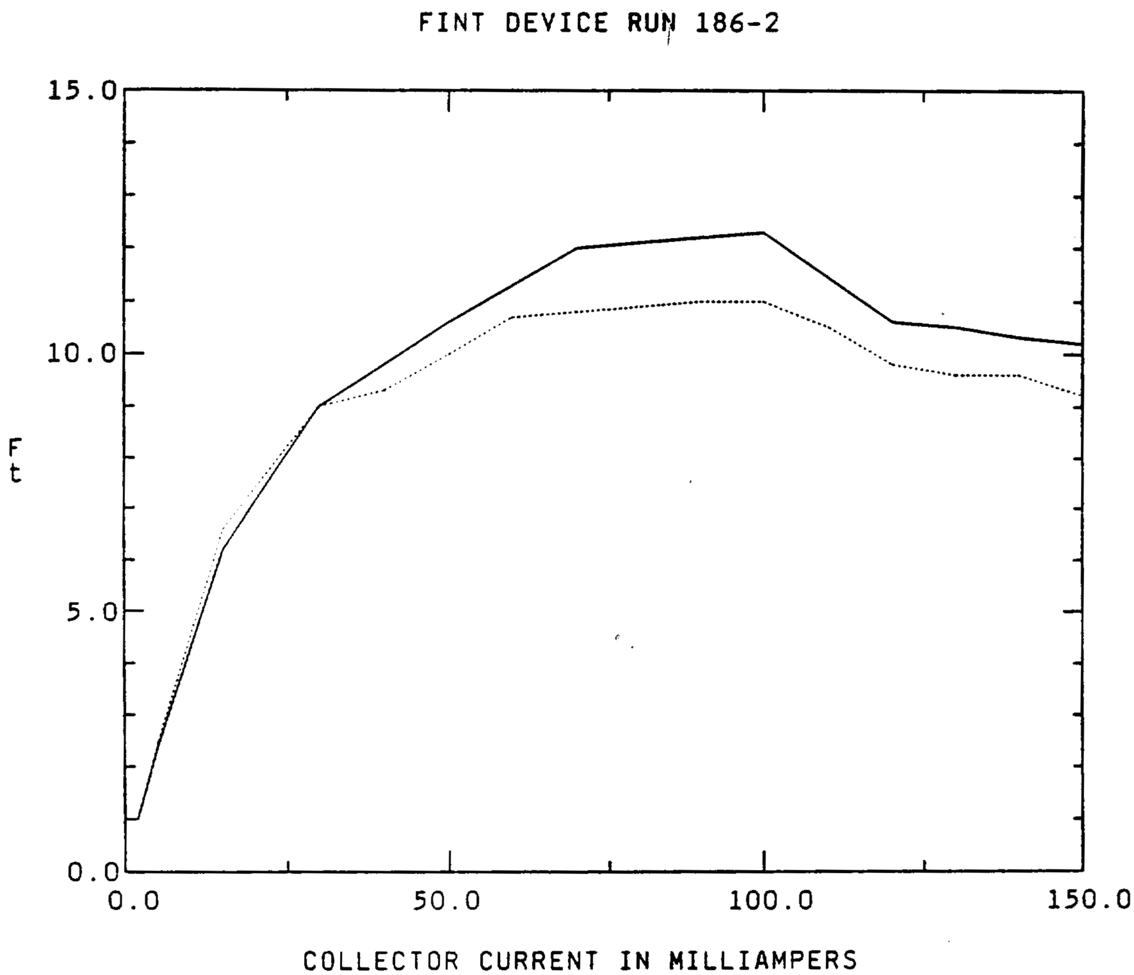

Figure B.3.3. f_T vs Collector Current, 3V, 4V

HIGH FREQUENCY PERFORMANCE OF HBT					
RUN	NAME	DEVICE	BIAS	FT	FMAX
189-3	b1	fin:	3v5ma	2.8	8.5
189-3	b1	fint	3v10ma	4.4	8.75
189-3	b1	fint	3v15ma	5.0	8.75
189-3	b1	fint	3v20ma	6.0	9.0
189-3	b1	fint	3v30ma	6.7	8.75
189-3	b1	fint	3v50ma	7.7	9.0
189-3	b2	fint	3v10ma	5.0	8.5
189-3	b2	fint	3v15ma	5.9	8.5
189-3	b2	fint	4v15ma	5.6	9.0
189-3	b2	fint	4v20ma	6.2	9.0
189-3	b2	fint	4v30ma	8.6	9.0
189-3	b2	fint	4v50ma	9.5	9.5
189-3	b3	4x10A	4v2ma	11.0	
189-3	b3	4x10A	4v5ma	2.5	11.0
189-3	b3	4x10A	4v10ma	2.7	11.0
189-3	b3	4x10A	4v15ma	3.0	11.0
189-3	b3	4x10A	4v20ma	3.2	11.0
189-3	b3	4x10A	4v30ma	2.9	11.0

Table B.4. Data Summary of Run 189-3, FINT

HIGH FREQUENCY PERFORMANCE OF HBT					
RUN	NAME	DEVICE	BIAS	FT	FMAX
210-1	j	fint	3v2ma	1.0	1.0
210-1	j	fint	3v5ma	3.4	1.7
210-1	j	fint	3v10ma	4.5	2.3
210-1	j	fint	3v15ma	5.6	2.7
210-1	j	fint	3v20ma	6.5	2.9
210-1	j	fint	3v25ma	7.2	2.9
210-1	j	fint	3v30ma	7.7	2.9
210-1	j	fint	3v35ma	7.9	3.2
210-1	j	fint	3v40ma	8.0	3.1
210-1	j	fint	3v45ma	8.3	3.3
210-1	j	fint	3v50ma	8.2	3.3

Table B.5.1. Data Summary of Run 210-1, FINT j

HIGH FREQUENCY PERFORMANCE OF HBT					
RUN	NAME	DEVICE	BIAS	FT	FMAX
210-1	k	fint	3v2ma	1.0	1.0
210-1	k	fint	3v5ma	2.5	4.2
210-1	k	fint	3v10ma	3.8	4.7
210-1	k	fint	3v15ma	5.7	5.1
210-1	k	fint	3v20ma	6.4	5.7
210-1	k	fint	3v25ma	7.5	5.7
210-1	k	fint	3v30ma	8.2	6.0
210-1	k	fint	3v35ma	8.8	6.1
210-1	k	fint	3v40ma	9.1	6.1
210-1	k	fint	3v45ma	9.6	6.2
210-1	k	fint	3v50ma	9.8	6.2
210-1	k	fint	3v55ma	10.0	6.2
210-1	k	fint	3v60ma	10.3	6.2
210-1	k	fint	3v65ma	10.4	6.2
210-1	k	fint	3v70ma	10.6	6.2
210-1	k	fint	3v75ma	10.8	6.2
210-1	k	fint	3v80ma	10.9	6.2
210-1	k	fint	3v85ma	10.8	6.2
210-1	k	fint	3v90ma	11.0	6.1
210-1	k	fint	3v95ma	11.0	6.1
210-1	k	fint	3v100ma	11.1	6.0
210-1	k	fint	3v110ma	11.3	6.1

Table B.5.2. Data Summary of Run 210-1, FINT k

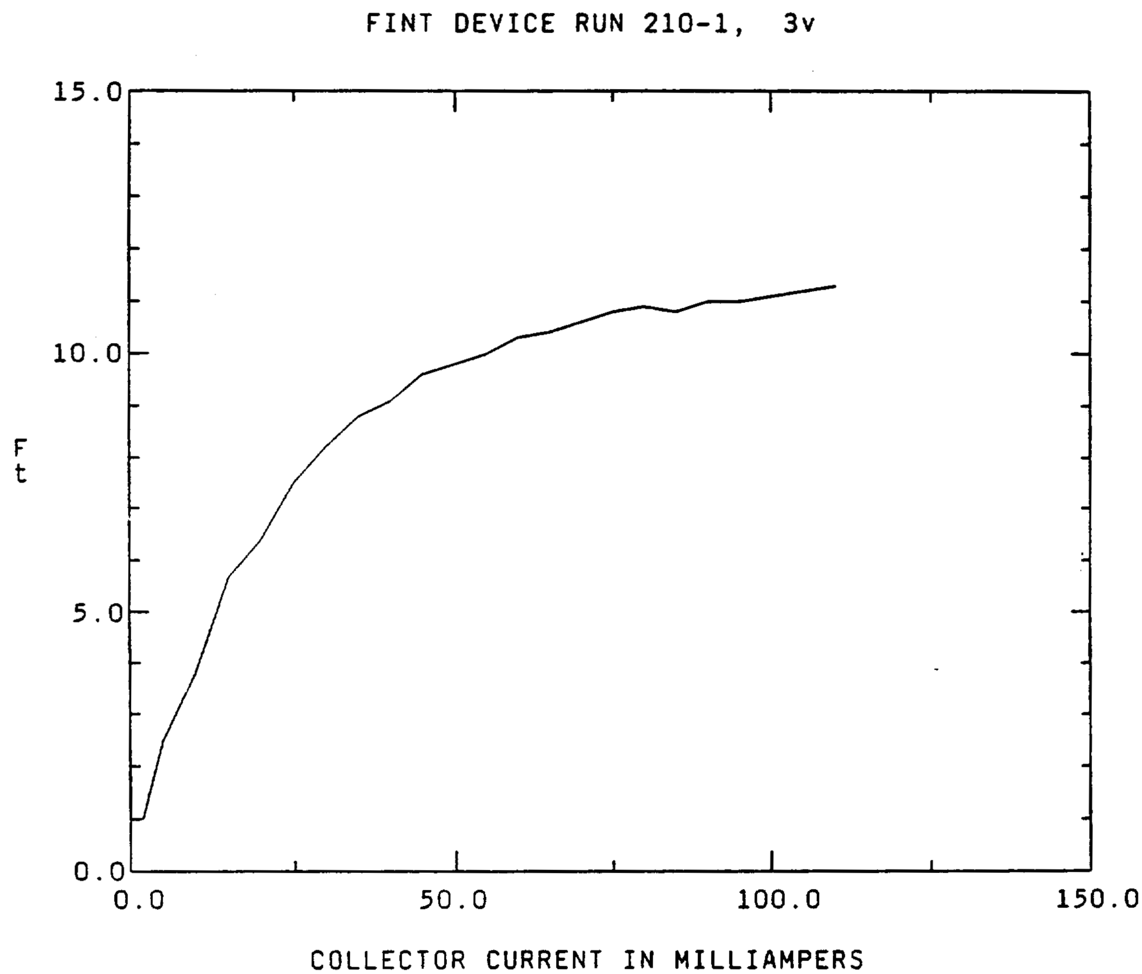

Figure B.5.2. f_T vs Collector Current, 3V

HIGH FREQUENCY PERFORMANCE OF HBT					
RUN	NAME	DEVICE	BIAS	FT	FMAX
210-4	1	fint	3v2ma	1.2	3.1
210-4	1	fint	3v5ma	2.5	4.4
210-4	1	fint	3v10ma	4.8	5.2
210-4	1	fint	3v15ma	6.7	5.8
210-4	1	fint	3v20ma	7.4	6.0
210-4	1	fint	3v25ma	8.5	6.2
210-4	1	fint	3v30ma	9.2	6.3
210-4	1	fint	3v35ma	10.8	6.5
210-4	1	fint	3v40ma	11.0	6.7
210-4	1	fint	3v45ma	11.6	6.7
210-4	1	fint	3v50ma	11.9	6.7
210-4	1	fint	3v55ma	12.4	6.7
210-4	1	fint	3v60ma	12.6	6.9

Table B.6.1. Data Summary of Run 210-4, FINT 3V

HIGH FREQUENCY PERFORMANCE OF HBT					
RUN	NAME	DEVICE	BIAS	FT	FMAX
210-4	1	fint	4v2ma	1.1	4.4
210-4	1	fint	4v5ma	2.6	4.5
210-4	1	fint	4v10ma	4.9	5.6
210-4	1	fint	4v15ma	6.5	6.1
210-4	1	fint	4v20ma	7.5	6.5
210-4	1	fint	4v25ma	8.6	6.8
210-4	1	fint	4v30ma	9.7	6.8
210-4	1	fint	4v35ma	10.2	7.0
210-4	1	fint	4v40ma	10.8	7.0
210-4	1	fint	4v45ma	11.1	7.2
210-4	1	fint	4v50ma	11.8	7.2
210-4	1	fint	4v55ma	12.1	7.2
210-4	1	fint	4v60ma	12.2	7.2
210-4	1	fint	4v65ma	12.5	7.4
210-4	1	fint	4v70ma	12.6	7.4
210-4	1	fint	4v75ma	12.8	7.4
210-4	1	fint	4v80ma	12.6	7.4
210-4	1	fint	4v85ma	12.6	7.4
210-4	1	fint	4v90ma	12.8	7.4
210-4	1	fint	4v95ma	12.7	7.4
210-4	1	fint	4v100ma	12.9	7.4
210-4	1	fint	4v105ma	12.8	7.4
210-4	1	fint	4v110ma	13.0	7.4
210-4	1	fint	4v115ma	12.6	7.4

Table B.6.2. Data Summary of Run 210-4, FINT 1 4V

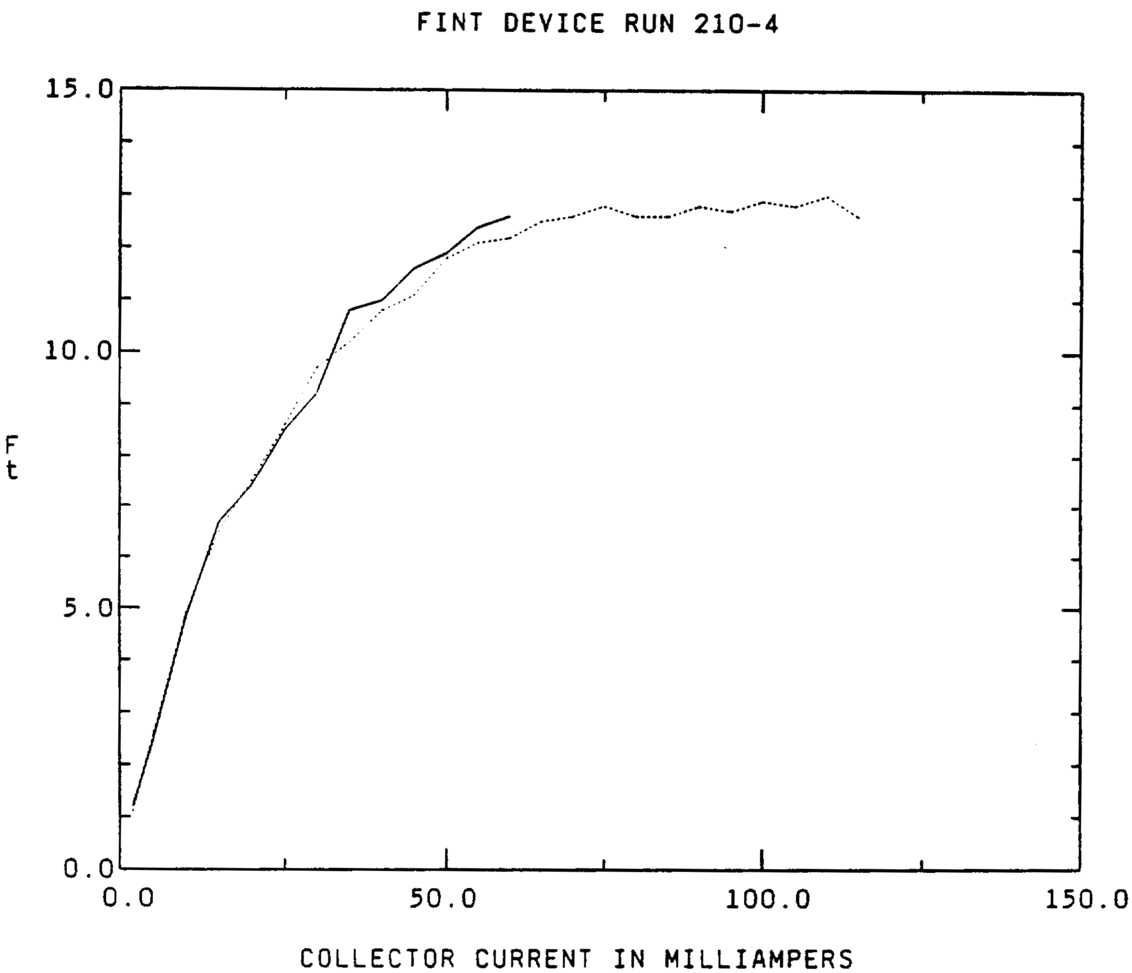

Figure B.6.2. f_T vs Collector Current, 3V, 4V

HIGH FREQUENCY PERFORMANCE OF HBT					
RUN	NAME	DEVICE	BIAS	FT	FMAX
211-1b	m	fint	3v2ma	1.2	2.1
211-1b	m	fint	3v5ma	2.5	3.0
211-1b	m	fint	3v10ma	4.9	3.9
211-1b	m	fint	3v15ma	6.7	4.3
211-1b	m	fint	3v20ma	7.1	4.7
211-1b	m	fint	3v25ma	8.0	4.8
211-1b	m	fint	3v30ma	9.9	4.9
211-1b	m	fint	3v35ma	10.7	5.0
211-1b	m	fint	3v40ma	10.2	5.1
211-1b	m	fint	3v45ma	11.6	5.3
211-1b	m	fint	3v50ma	12.0	5.3
211-1b	m	fint	3v55ma	12.4	5.3
211-1b	m	fint	3v60ma	12.7	5.3
211-1b	m	fint	3v65ma	13.0	5.4
211-1b	m	fint	3v70ma	12.2	5.4
211-1b	m	fint	3v75ma	13.4	5.4
211-1b	m	fint	3v80ma	13.7	5.4
211-1b	m	fint	3v85ma	13.6	5.4
211-1b	m	fint	3v90ma	13.8	5.4
211-1b	m	fint	3v95ma	14.0	5.4
211-1b	m	fint	3v100ma	14.2	5.4
211-1b	m	fint	3v105ma	14.1	5.4
211-1b	m	fint	3v110ma	14.0	5.4
211-1b	m	fint	3v115ma	14.0	5.4

Table B.7. Data Summary of Run 211-1b, FINT

APPENDIX C: SIM Users Guide

SIM is a program that was designed as a tool to extract frequency vs gain values, and print these values in tabular form. These tables can then be examined to yield f_T and $f_{\max}$ estimates. The program assumes the data was taken in the common-collector (*CC*) orientation and with the ports reversed, i.e. emitter port 1 and base port 2. This is the experimental orientation dictated by the physical layout of the device bonded to the hybrid test structure. Input data is expected to be in this orientation and translated to base port 1, common-emiter configuration.

With *SIM* resident in the same directory as the *CC*, base port 2 data, it can be invoked by typing *SIM* at the system prompt. A menu is displayed on the screen, describing each *option.* on the data. An output file is created as a *fn.out* file and results can be directed to this file if so chosen as output destination. This file will exist at the invoking of *SIM*, regardless.

To read the data file, selection of *option* 1 will prompt the user for the complete name of the data file.

The computation of all gains are performed in the common-emitter mode. To change the data file to common-emitter, base port 1 mode, select *option* 3. A data file is then created containing the data in the proper format. The original data file is left unaltered.

Frequency vs. β(db); β; and *frequency* * β, can be obtained by the selection of *option* 4.

Generation of *Maximum Availible Gain*(db) vs. *Frequency* and *Unilateral-PowerGain* vs. *Frequency* are produced by the selection of *option* 5 and 6. These *options* will prompt the user for the direction of output and the number of frequency points of interest.

The extraction of hybrid-π model circuit parameters is not completely implemented. However, some information can be derived by invoking *option* 7 and following the prompts.

The parasitic pad capacitances can degrade the values determined by *SIM* unless they are de-embedded from the data. *Option* 8 uses the *CC* data and prompts the user for the values in, femto-farads, of the port pad capacitances. Using standard transformations to *ABCD* matrices and analysis, the pads are removed from the data. The *CC* data file is then returned to the main program ready to be manipulated. It should be noted that this function changes only the original *CC* file and needs to be translated into *CE* in the manner described previously.

Options 2 and 9 are intended to be de-bugging tools as well as provide access to the data during the running of *SIM*. The *CC* data is echoed by *option* 2 and *CE* data by *option* 9. Both outputs are in polar form.

When a large number of data files need to be analyzed for f_T and $f_{\max}$, *option* 10 is very helpful. This *option* performs the entire analysis on the data from changing the data to *CE*, to printing the Unilateral Power Gain file. The sequence it follows is: 3, 4, 5, 6, 11. It then returns expecting the next file name to be entered. The user merely answers the prompt once for the file direction and the number of data points need for each analysis. This *option* allows the user to perform analysis on many data files very quickly. Termination of the program from *option* 10 requires the input of a non-existent or a prior input data file.

Selection of *option* 11 from the menu prompt will read in additonal data files and *option* 12 allows the program to gracefully terminate.

```
c       ***************************************************************
c       SIM PROGRAM
c       ***************************************************************
c       ***************************************************************
c       HELP FILE
c       ***************************************************************
        subroutine Header
        write(6,*)'***************************************************'
        write(6,*)'This program is designed to use common-'
        write(6,*)'collector s-parameter data as input assuming the'
        write(6,*)'emitter is port 1 and the base is port 2. This is'
        write(6,*)'non-standard, but the way the HBT devices are measured.'
        write(6,*)'The figures of merit that this program intends to deliver'
        write(6,*)'are: ft, beta(db), f*beta, hre, Maximum Available Gain'
        write(6,*)'(Gamax). Ft will be calculated using the h21 and the '
        write(6,*)'common-collector s21/s12 methods.'
        write(6,*)'This program was written by: Jim Mattern 7/1/88'
        write(6,*)
        write(6,*)'The method:'
                write(6,*)'initialize constants'
                write(6,*)'read in s-parameter data'
                write(6,*)'exchange ports: emitter to port 2, base port 1'
                write(6,*)'translate common-collector s-pars{sc} to y-pars{yc}'
                write(6,*)'translate common-collector y-pars{yc} to common-'
                write(6,*)'emitter y-pars{ye}'
                write(6,*)'calculate common-collector beta(|s21/s12|){ccbeta}'
                write(6,*)'calculate common-emitter beta(|y21/y11|){cebeta}'
                write(6,*)'calculate common-emitter hre(|y12/y11|){hre}'
                write(6,*)'calculate Maximum Stable Gain {Gmsg}'
                write(6,*)'calculate Maximum Available Gain {Gmag}'
                write(6,*)'calculate Unilateral Gain {Gug}'
                write(6,*)'ccbeta, ccbeta(db), f*ccbeta, hre'
                write(6,*)'cebeta, cebeta(db), f*cebeta, Gamax'
        return
        end
c       ************************************************
c       MAIN SIM PROGRAM
c       ************************************************
        implicit double precision (a-h,o-z)
        complex sc(2,2,201)
        complex se(2,2,201)
        character*32,ifile,ofile
        character*79 head(9)
        integer n, nfreq,device
        integer comemitter,rectangular
        real freq(201)
        nfreq=0
        comemitter = 0
```

```
        rectangular = 0
2       call select(n)
        go to (10,20,30,40,50,60,70,80,90,100,130,140), n
c       ************************************************
10      call readsfile(ifile,ofile,sc,nfreq,freq,head)
c       ************************************************
        comemitter = 0
        rectangular = 0
        go to 2
20      continue
                call prompt(device)
c       ************************************************
                call mpwrite(ifile,head,sc,nfreq,freq,device)
c       ************************************************
                go to 2
30      call cctoce(sc,se,nfreq,device)
        comemitter=1
        rectangular=1
                go to 2
40      if ((comemitter.eq.1).and.(rectangular.eq.1)) then
45              call prompt(device)
c       ************************************************
                call ft(se,freq,nfreq,device,ifile)
c       ************************************************
                go to 2
        else if (comemitter.eq.1) then
                go to 148
        else
                go to 145
        end if
50      if ((comemitter.eq.1).and.(rectangular.eq.1)) then
55              call prompt(device)
c       ************************************************
                call  gains(se,freq,nfreq,device)
c       ************************************************
                go to 2
        else if (comemitter.eq.1) then
                go to 148
        else
                go to 145
        end if
60      if ((comemitter.eq.1).and.(rectangular.eq.1)) then
65              call prompt(device)
c       ************************************************
                call  ungain(se,freq,nfreq,device)
c       ************************************************
                go to 2
        else if (comemitter.eq.1) then
```

```
                  go to 148
          else
                  go to 145
          end if
70        call prompt(device)
c         ************************************************
          call  element(sc,freq,nfreq,device)
c         ************************************************
                  go to 2
80        call prompt(device)
c         ************************************************
          call  deembed(sc,freq,nfreq,device)
c         ************************************************
                  go to 2
90        continue
                  call prompt(device)
                  call rectomag(se,nfreq,dev)
c         ************************************************
                  call mpwrite(ifile,head,se,nfreq,freq,device)
c         ************************************************
                  go to 2
100     continue
                  call prompt(device)
101       call cctoce(sc,se,nfreq,device)
          comemitter=1
          rectangular=1
                  call ft(se,freq,nfreq,device,ifile)
                  call  gains(se,freq,nfreq,device)
                  call  ungain(se,freq,nfreq,device)
          call readsfile(ifile,ofile,sc,nfreq,freq,head)
          comemitter = 0
          rectangular = 0
                  go to 101
130       close(2,STATUS='KEEP')

          go to 10
145     write(6,*)'common-collector configuration is unacceptable.'
          write(6,*)'translate to common-emitter.'
          go to 2
146       write(6,*)'the parameters are in real and imaginary form.'
          write(6,*)'please translate to magnitude and angle.'
          go to 2
147       write(6,*)'the parameters are in common-emiter configuration'
          write(6,*)'please translate to common-collector.'
          go to 2
148       write(6,*)'the parameters are in magtnitude and phase.'
          write(6,*)'please translate to rectangular.'
          go to 2
```

```
140     STOP
221     format(1x,'Y-parameters: ',a//)
222    format('freq',17x,'Y11/Y21',29x,'Y12/Y22')
223    format(2x,'GHz',11x,'RE',12x,'IM',26x,'RE',12x,'IM')
321     format(1x,'S-parameters: ',a//)
322    format('freq',17x,'S11/S21',29x,'S12/S22')
        END

        subroutine prompt(dev)
        integer dev,n
10      write(6,*)'print to screen(6) or file(2)'
        read *,n
        if (n.eq.6) then
                dev= 6
        else if (n.eq.2) then
                dev= 2
        else
                go to 10
        end if
        return
        end


        FUNCTION CANG(W)
        COMPLEX W
        X = REAL(W)
        Y = AIMAG(W)
        CANG=ATAN2(Y,X)
        RETURN
        END


        FUNCTION ANG(RAD)
        PI = 4.*atan(1.)
        ANG = RAD * 180/PI
        RETURN
        END


        FUNCTION RAD(ANG)
        PI = 4.*atan(1.)
        RAD = ANG * PI/180
        RETURN
        END
c       ****************************************************************
c       TRANSLATE ABCD to S PARAMETERS
c       ****************************************************************
        subroutine abcdtos(a,s,nf,dev)
```

```
        complex s(2,2,201)
        complex a(2,2,201)
        complex Ap,Bp,Cp,Dp
        complex deltas
        integer i,nf,dev
        real zo
        zo=50.
        write(dev,*)' translating from ABCD pars to s pars'
        do 200 i = 1,nf
                Ap=a(1,1,i)
                Bp=a(1,2,i)/zo
                Cp=a(2,1,i)*zo
                Dp=a(2,2,i)
                deltas =Ap+Bp+Cp+Dp
                s(1,1,i)=(Ap+Bp-Cp-Dp)/deltas
                s(1,2,i)= 2.*(Ap*Dp-Bp*Cp)/deltas
                s(2,1,i)= 2./deltas
                s(2,2,i)=(-Ap+Bp-Cp+Dp)/deltas
200     continue
        return
        end
c       *************************************************************
c       PRINT FILE of GAIN  vs FREQUENCY
c       *************************************************************
        subroutine betawrite(ifile,rf,beta,db,nf,dev)
        real rf(201)
        real beta(201)
        real db(201)
        character*32, ifile
        integer i,nf,k,dev,step
        write(6,*)'number of points?'
        read *,k
        if (k.lt.nf) then
                step = nf/k
        else
                step = 1
        end if
        write(dev,*)
 100    write(dev,101)ifile
 101    format(1x,'File: ',a//)
        write(dev,102)
        do 200 i=1,nf,step
c     write(dev,199)rf(i)*1e9,db(i),beta(i),rf(i)*beta(i)
                write(dev,199)rf(i)*1e9,db(i)
 200    continue
 102    format(4x,'f',17x,'beta(db)')
c102    format(4x,'f',17x,'beta(db)',12x,'beta',15x,'f*beta')
c199   format(e10.4,7x,f12.4,7x,f12.4,7x,f12.4)
```

```
199     format(e10.4,7x,f12.4)
        return
        end
c       **************************************************************
c       COMMON-COLLECTOR to COMMON-EMITTER
c       **************************************************************
        subroutine cctoce(s1,s2,nf,dev)
        complex y(2,2,201)
        complex s1(2,2,201)
        complex s2(2,2,201)
        complex a(2,2,201)
        complex y11,y22,y12,y21
        integer nf,dev
        write(dev,*)' exchanging ports'
        do 120 i=1,nf
                a(1,1,i)=s1(2,2,i)
                a(2,1,i)=s1(1,2,i)
                a(1,2,i)=s1(2,1,i)
                a(2,2,i)=s1(1,1,i)
120     continue
        call magtorec(a,nf,dev)
        call spartoypar(a,y,nf,dev)
        write(dev,*)' translated to common-emitter yparameters'
        write(dev,*)
        do 220 i=1,nf
                y22=y(1,1,i)+y(2,2,i)+y(2,1,i)+y(1,2,i)
                y12=-y(1,1,i)-y(1,2,i)
                y21=-y(1,1,i)-y(2,1,i)
                y11= y(1,1,i)
                y(1,1,i)=y11
                y(1,2,i)=y12
                y(2,1,i)=y21
                y(2,2,i)=y22
220     continue
        call ypartospar(y,s2,nf,dev)
        return
        end
c       **************************************************************
c       COMMON-EMITTER to COMMON-COLLECTOR
c       **************************************************************
        subroutine cetocc(s1,s2,nf,dev)
        complex y(2,2,201)
        complex s1(2,2,201)
        complex s2(2,2,201)
        complex a(2,2,201)
        complex y11,y22,y12,y21
        integer nf,dev
        call magtorec(s1,nf,dev)
```

```
      call spartoypar(s1,y,nf,dev)
      write(dev,*)' translated to common-collector yparameters'
      write(dev,*)
      do 120 i=1,nf
            y22=y(1,1,i)+y(2,2,i)+y(2,1,i)+y(1,2,i)
            y12=-y(1,1,i)-y(1,2,i)
            y21=-y(1,1,i)-y(2,1,i)
            y11= y(1,1,i)
            y(1,1,i)=y11
            y(1,2,i)=y12
            y(2,1,i)=y21
            y(2,2,i)=y22
120   continue
      call ypartospar(y,s2,nf,dev)
      write(dev,*)' exchanging ports'
      do 220 i=1,nf
            a(1,1,i)=s2(2,2,i)
            a(2,1,i)=s2(1,2,i)
            a(1,2,i)=s2(2,1,i)
            a(2,2,i)=s2(1,1,i)
            s2(1,1,i)=a(1,1,i)
            s2(1,2,i)=a(1,2,i)
            s2(2,2,i)=a(2,2,i)
            s2(2,2,i)=a(2,2,i)
220   continue
      call rectomag(s2,nf,dev)
      return
      end
c     ************************************************************
c     DE-EMBED PARASITICS
c     ************************************************************
      subroutine deembed(s,rf,nf,dev)
      complex s(2,2,201)
      complex A(2,2,201)
      complex B(2,2,201)
      complex y1,y2,Am,Bm,Cm,Dm
      real rf(201),p,q,omega
      integer nf,dev,i
      pi = 4.*atan(1.)
      write(6,*)' input dc value of emitter parasitic capacitor in F-Farads '
      read *,p
      p=p*(1.e-15)
      write(dev,*)'Zemitter = ',p,' farads'
      write(6,*)' input dc value of base parasitic capacitor in F-Farads '
      read *,q
      q=q*(1.e-15)
      write(dev,*)'Zbasepar = ',q,' farads'
      call magtorec(s,nf,dev)
```

```
      call stoabcd(s,A,nf,dev)
      write(dev,*)' de-embedded spars'
      do 120 i=1,nf
            omega = 2.*pi*rf(i)*1e9
            y1 = cmplx(0,p*omega)
            y2 = cmplx(0,q*omega)
            Am = A(1,1,i)
            Bm = A(1,2,i)
            Cm = A(2,1,i)
            Dm = A(2,2,i)
            B(1,1,i) = Am-Bm*y2
            B(1,2,i) = Bm
            B(2,1,i) = Bm*y1*y2 -Am*y1-Dm*y2 +Cm
            B(2,2,i) = Dm - Bm*y1
120   continue
      call abcdtos(B,s,nf,dev)
      call rectomag(s,nf,dev)
      write(dev,*)
      return
      end
c     **************************************************************
c     Ft
c     **************************************************************
      subroutine ft(s,freq,nfreq,dev,ifile)
      complex y(2,2,201)
      complex s(2,2,201)
      real beta(201),db(201),freq(201)
      integer i,nfreq,dev
      call spartoypar(s,y,nfreq,dev)
      write(dev,*)'ft from common emitter y parameters'
      do 200 i=1,nfreq
            beta(i)=abs(y(2,1,i)/y(1,1,i))
            db(i)=20*log10(beta(i))
200   continue
      call betawrite(ifile,freq,beta,db,nfreq,dev)
      call ypartospar(y,s,nfreq,dev)
      return
      end
c     **************************************************************
c     POWER GAIN
c     **************************************************************
      subroutine gains(s,rf,nf,dev)
      complex s11,s12,s21,s22
      complex s(2,2,201)
      complex delta
      real rf(201)
      real ak, dm
      integer dev,i,nf,step,k
```

```
        write(dev,*)' power gain calculations '
        write(6,*)'number of points?'
        read *,k
        if (k.lt.nf) then
                step = nf/k
        else
                step = 1
        end if
        write(dev,*)
        write(dev,102)
102     format(4x,'f',17x,'GMSG(DB)')
        do 200 i=1,nf,step
                s11 = s(1,1,i)
                s12 = s(1,2,i)
                s21 = s(2,1,i)
                s22 = s(2,2,i)
                if (s12.eq.0.0) go to 2999
                delta= s11*s22 - s12*s21
                dm = cabs(delta)
                h1 = cabs(s21*s12)
                if (h1.eq.0.) go to 230
                        ak = (1-cabs(s11)**2-cabs(s22)**2 + dm**2)/(2*h1)
                        go to 300
230             ak = 1e10
300             if ((ak.gt.1.).and.(dm.lt.1.)) go  to 2093
                gmsg = cabs(s21/s12)
                gmsg = 10*ALOG10(gmsg)
                write(dev,199)rf(i)*1e9,gmsg
c               write(dev,*)rf(i)*1e9,'HZ POTENT UNSTAB, GMSG = ',gmsg,'DB'
                go to 200
2093    GPMAX =(ak-SQRT(ak**2-1))*CABS(s21/s12)
        GPMAX = 10*ALOG10(GPMAX)
c       write(dev,*)rf(i)*1e9,'HZ UNCOND. STABLE GPMAX = ',GPMAX,'DB'
        write(dev,*)rf(i)*1e9,GPMAX
199     format(e10.4,7x,f12.4)
200     continue
        return
2999    write(dev,*)' *********** S12 EQUALS ZERO ...ERRR ****'
        return
        end
c       **************************************************************
c       POLAR TO RECTANGULAR
c       **************************************************************
        subroutine magtorec(s,nf,dev)
        complex s(2,2,201)
        real s11m,s11a,s12m,s12a,s21m,s21a,s22m,s22a
        integer i,nf,dev
        write(dev,*)' transposed to rectangular coordinates'
```

```
        rflag = 1
        do 100 i=1,nf
                s11m= real(s(1,1,i))
                s11a= aimag(s(1,1,i))
                s21m= real(s(2,1,i))
                s21a= aimag(s(2,1,i))
                s12m= real(s(1,2,i))
                s12a= aimag(s(1,2,i))
                s22m= real(s(2,2,i))
                s22a= aimag(s(2,2,i))
                s(1,1,i)=cmplx(s11m* COS(RAD(s11a)), s11m* SIN(RAD(s11a)))
                s(1,2,i)=cmplx(s12m* COS(RAD(s12a)), s12m* SIN(RAD(s12a)))
                s(2,1,i)=cmplx(s21m* COS(RAD(s21a)), s21m* SIN(RAD(s21a)))
                s(2,2,i)=cmplx(s22m* COS(RAD(s22a)), s22m* SIN(RAD(s22a)))
100     continue
        return
        end
c       ************************************************************
c       ECHO data  to file *.out
c       *************************************************************
        subroutine mpwrite(ifile,head,s,nf,rf,dev)
        complex s(2,2,201)
        character*32,ifile
        character*79 head(9)
        real rf(201)
        integer i,nf,dev
                        write(dev,31)ifile
                        do 35 i = 1,9
                                write(dev,2)head(i)
35                      continue
                        do 50 i=1,nf
                          write(dev,40)rf(i),real(s(1,1,i)),aimag(s(1,1,i)),
     x            real(s(2,1,i)),aimag(s(2,1,i)),
     x            real(s(1,2,i)),aimag(s(1,2,i)),
     x            real(s(2,2,i)),aimag(s(2,2,i))
50                      continue
2     format(a79)
31      format(1x,'File: ',a//)
40      format(f7.4,'GHz',1x,f8.4,1x,f6.1,1x,f8.4,1x,f6.1,
     x          1x,f8.4,1x,f6.1,1x,f8.4,1x,f6.1)
        return
        end
c       ***********************************************************
c       READ s-parameter file
c       ***********************************************************
        subroutine readsfile(ifile,ofile,s,nf,rf,head)
        complex s(2,2,201)
        character*32,ifile,ofile
```

```
      character*79 head(9)
      real s11M,s11A,s12M,s12A,s21M,s21A,s22M,s22A
      real rf(201)
      integer i,nf
      print 1,'Enter input file name: '
      read(*,'(a)'),ifile
      ii=index(ifile,' ')-1
      ofile=ifile(1:ii)//'.out'
      open(unit=1,file=ifile,status='OLD',err=900)
      open(unit=2,file=ofile,status='NEW',err=999)
      do 5 i=1,9
            read(1,2,end=10),head(i)
 5    continue
      nf = 0
 10         continue
            i=nf+1
c     **********************************************
c     READ the data in polar form
c     **********************************************
            read(1,*,end=20),rf(i),s11M,s11A,s21M,s21A,s12M,s12A,s22M,s22A
            s(1,1,i)=cmplx(s11M,s11A)
            s(2,1,i)=cmplx(s21M,s21A)
            s(1,2,i)=cmplx(s12M,s12A)
            s(2,2,i)=cmplx(s22M,s22A)
            nf=nf+1
            go to 10
 20   continue
1     format(1x,a,x)
2     format(a79)
      return
900   print*,ifile,' -- file not found  (misspelled?)!)'
      stop
999   print*,ofile,' -- file specified exists!! restart   (DORK!)'
      stop
      end
c     ****************************************************************
c     RECTANGULAR TO POLAR
c     ****************************************************************
      subroutine rectomag(s,nf,dev)
      complex s(2,2,201)
      complex s11,s12,s21,s22
      integer i,nf,dev
      write(dev,*)' transposed to mag and angle coordinates'
      rflag = 0
      do 100 i=1,nf
            s11 = s(1,1,i)
            s12 = s(1,2,i)
            s21 = s(2,1,i)
```

```
            s22 = s(2,2,i)
            s(1,1,i)=cmplx(cabs(s11),ang(cang(s11)))
            s(1,2,i)=cmplx(cabs(s12),ang(cang(s12)))
            s(2,1,i)=cmplx(cabs(s21),ang(cang(s21)))
            s(2,2,i)=cmplx(cabs(s22),ang(cang(s22)))
100   continue
      return
      end
c     ************************************************************
c     ECHO the output file *.out
c     ************************************************************
      subroutine riwrite(dev,s,rf,nf)
      complex s(2,2,201)
      real rf(201)
      integer i,nf,dev
                  write(dev,223)
                  write(dev,*)
      do 400 i=1,nf
            write(dev,196)rf(i),real(s(1,1,i)),aimag(s(1,1,i)),
   x          real(s(1,2,i)),aimag(s(1,2,i))
            write(dev,198)real(s(2,1,i)),aimag(s(2,1,i)),
   x          real(s(2,2,i)),aimag(s(2,2,i))
196   format(f7.4,1x,f12.7,5x,f12.7,9x,f12.7,5x,f12.7)
198  format(8x,f12.7,5x,f12.7,9x,f12.7,5x,f12.7)
223  format(2x,'GHz',11x,'RE',12x,'IM',16x,'RE',12x,'IM')
400   continue
      return
      end
c     ************************************************************
c     SWITCH
c     ************************************************************
      SUBROUTINE SELECT (N)
      WRITE(6,*)
      WRITE(6,*)
      WRITE(6,11)
11    FORMAT("     ENTER:  1 to read in a S-parameter file",/
   1"         2 to echo common collector s-par data file in polar form",/
   2"         3 to translate common-collector to emitter"/
   3"         4 to calculate f vs beta",/
   4"         5 to calculate MAG or MSG ",/
   5"         6 to calculate Unilateral Power Gain ",/
   6"         7 to calculate intrinsic elements ",/
   7"         8 to de-embed the parasitics",/
   9"         9 to echo the common emitter s-par data file in polar form",/
   8"         10 to produce ce,ft,mag,ugain file",/
   8"         11 to read a new s parameter file",/
   9"         12 to exit")
```

```
      READ *,N
      RETURN
      END
c     ***************************************************************
c     TRANSLATE s-pars to ypars
c     ***************************************************************
      subroutine spartoypar(s,y,nf,dev)
      complex s(2,2,201)
      complex y(2,2,201)
      complex s11,s12,s21,s22
      complex deltas
      integer i,nf,dev
      real zo
      zo=50.
      write(dev,*)' translating from s pars to y pars'
      do 200 i = 1,nf
            s11=s(1,1,i)
            s12=s(1,2,i)
            s21=s(2,1,i)
            s22=s(2,2,i)
            deltas =(1.+s11)*(1.+s22)-s12*s21
            y(1,1,i)=((1.-s11)*(1.+s22)+s12*s21)/(zo*deltas)
            y(1,2,i)= -2.*s12/(zo*deltas)
            y(2,1,i)= -2.*s21/(zo*deltas)
            y(2,2,i)=((1.+s11)*(1.-s22)+s12*s21)/(zo*deltas)
200   continue
      return
      end
c     ***************************************************************
c     TRANSLATE s-pars to zpars
c     ***************************************************************
      subroutine spartozpar(s,z,nf,dev)
      complex s(2,2,201)
      complex z(2,2,201)
      complex s11,s12,s21,s22
      complex deltas
      integer i,nf,dev
      real zo
      zo=50.
      write(dev,*)' translating from s pars to z pars'
      do 200 i = 1,nf
            s11=s(1,1,i)
            s12=s(1,2,i)
            s21=s(2,1,i)
            s22=s(2,2,i)
            deltas =(1.-s11)*(1.-s22)-s12*s21
            z(1,1,i)=((1.+s11)*(1.-s22)+s12*s21)*zo/deltas
            z(1,2,i)= 2.*s12*zo/deltas
```

```
          z(2,1,i)= 2.*s21*zo/deltas
          z(2,2,i)=((1.-s11)*(1.+s22)+s12*s21)*zo/deltas
200    continue
       return
       end
c      ***********************************************************
c      TRANSLATE s-pars to ABCD
c      ***********************************************************
       subroutine stoabcd(s,a,nf,dev)
       complex s(2,2,201)
       complex a(2,2,201)
       complex s11,s12,s21,s22
       complex deltas
       integer i,nf,dev
       real zo
       zo=50.
       write(dev,*)' translating from s pars to ABCD pars'
       do 200 i = 1,nf
          s11=s(1,1,i)
          s12=s(1,2,i)
          s21=s(2,1,i)
          s22=s(2,2,i)
          deltas =2.*s21
          a(1,1,i)=((1.+s11)*(1.-s22)+s12*s21)/deltas
          a(1,2,i)= ((1.+s11)*(1.+s22)-s12*s21)*zo/deltas
          a(2,1,i)= ((1.-s11)*(1.-s22)-s12*s21)/(deltas*zo)
          a(2,2,i)=((1.-s11)*(1.+s22)+s12*s21)/deltas
200    continue
       return
       end
c      ***********************************************************
c      UNITY GAIN
c      ***********************************************************
       SUBROUTINE UNGAIN (s,rf,nf,dev)
       COMPLEX s11,s21,s22,s(2,2,201)
       real rf(201)
       integer i,nf,dev,k,step
       write(dev,*)
       write(dev,*)' Unity gain'
       write(6,*)'number of points?'
       read *,k
       if (k.lt.nf) then
          step = nf/k
       else
          step = 1
       end if
       write(dev,102)
102    format(4x,'f',17x,'uGAIN(DB)')
```

```
      do 7002 i = 1,nf,step
            s11=s(1,1,i)
            s12=s(1,2,i)
            s21=s(2,1,i)
            s22=s(2,2,i)
            IF ((CABS(s11) .GE.1.) .OR. ( CABS(s22).GE.1.)) GO TO 7082
            GSM = 10*ALOG10(1/(1-CABS(s11)**2))
            GLM = 10*ALOG10(1/(1-CABS(s22)**2))
            GO = 10*ALOG10(CABS(s21)**2)
            GUMAX = GSM+GLM+GO
            write(dev,199)rf(i)*1e9,GUMAX
c           write(dev,*)rf(i)*1e9,'GHz    GTUMAX(DB)= ',GUMAX
            GO TO 7002
7082  write(dev,*)rf(i), '   POTENTIALLY UNSTABLE TRANSISTOR  '
199   format(e10.4,7x,f12.4)
7002  continue
7092  RETURN
      END
c     ************************************************************
c     TRANSLATE ypars to spars
c     ************************************************************
      subroutine ypartospar(y,s,nf,dev)
      complex s(2,2,201)
      complex y(2,2,201)
      complex y11,y12,y21,y22
      complex deltas
      integer i,nf,dev
      real zo
      zo=50.
      write(dev,*)' translating from y pars to s pars'
      do 200 i = 1,nf
            y11=y(1,1,i)*zo
            y12=y(1,2,i)*zo
            y21=y(2,1,i)*zo
            y22=y(2,2,i)*zo
            deltas =(y11 + 1.)*(y22 +1.) - y21*y12
            s(1,1,i)=((1.-y11 )*(1.+y22 ) + y21*y12)/deltas
            s(2,2,i)=((1.+y11 )*(1.-y22 ) + y21*y12)/deltas
            s(1,2,i)= -2.*y12/deltas
            s(2,1,i)= -2.*y21/deltas
200   continue
      return
      end
c     *************************************************************
c     TRANSLATE y-pars to z-pars
c     *************************************************************
      subroutine ypartozpar(y,z,nf,dev)
      complex y(2,2,201)
```

```
      complex z(2,2,201)
      complex y11,y12,y21,y22
      complex deltas
      integer i,nf,dev
      real zo
      zo=50.
      write(dev,*)' translating yparameters to z parameters'
      do 200 i = 1,nf
            y11=y(1,1,i)/zo
            y12=y(1,2,i)/zo
            y21=y(2,1,i)/zo
            y22=y(2,2,i)/zo
            deltas =abs(y11*y22-y12*y21)
            z(1,1,i)=y22/deltas
            z(1,2,i)= -y12/deltas
            z(2,1,i)= -y21/deltas
            z(2,2,i)=y11/deltas
200   continue
      return
      end
c     ***************************************************************
c     TRANSLATE z-pars to y-pars
c     ***************************************************************
      subroutine zpartoypar(z,y,nf,dev)
      complex z(2,2,201)
      complex y(2,2,201)
      complex z11,z12,z21,z22
      complex deltas
      integer i,nf,dev
      real zo
      zo=50.
      write(dev,*)' translating zpars to ypars'
      do 200 i = 1,nf
            z11=z(1,1,i)*zo
            z12=z(1,2,i)*zo
            z21=z(2,1,i)*zo
            z22=z(2,2,i)*zo
            deltas = z11*z22-z12*z21
            y(1,1,i)=  z22/(deltas)
            y(1,2,i)= -z12/(deltas)
            y(2,1,i)= -z21/(deltas)
            y(2,2,i)=  z11/(deltas)
200   continue
      return
      end
```

```
c     This program is brought to you by JAMES W. MATTERN OF OGC
c
c     initializing
c
      real   Lt,Le,ni,k,Ic,Nde,Ndc,Nab
      open(3,FILE="theory")
      We0  = 0.1e-6
      We1  = 0.125e-6
      We2  = 0.25e-6
      We   = We0 + We1 + We2
      Wb   = 0.1e-6
      Wc   = 0.7e-6
      Dpe  = 5
      Dnb  = 50
      upe  = 200
      unb  = 2000
      ni = 2.25e6
      es = 1.17e-12
      k = 1.38-23
      T = 300
      q = 1.6e-19
      Vt = 0.02589
100   print *,'input the RUN number '
      read *,RUN
      print *,'input the Emitter doping concentration Nde (cm-3)'
      read *,Nde
      print *,'input the Base doping concentration Nab(cm-3)'
      read *,Nab
      print *,'input the Collector doping concentration Ndc (cm-3)'
      read *,Ndc
      print *,'input the resistivity of GaAs emitter rowE1 (ohm-cm)'
      read *,rowE1
      rowE2 = 6.25e-3
      print *,'input the sheet resistance of intrinsic base rowIB (ohm/sq)'
      read *,rowIB
      print *,'input the sheet resistance of extrinsic base rowXB (ohm/sq)'
      read *,rowXB
      print *,'input the calculated pad capacitance Cpad (farads)'
      read *,Cpad
      rowC  = 6e-2
c     For a mesa etched process rowIB~= rowXB
      rowSK = 2*rowXB
      rowCn = 1e-6
      print *,'input the p-type specific contact resistivity rowCp (ohmcm^2)'
      read *,rowCp
      Lt    = ((rowCP/rowSK)**0.5)*1e4
      print *,'input the area of the emitter Ae (um^2) '
      read *,Ae
```

```
print *,'input the area of the collector Ac (um^2)'
read *,Ac
Se = 4
print *,'input the length of the emitter finger Le (um)'
read *,Le
print *,'input the base stripe width(um) Sb '
read *,Sb
print *,'input the emitter-base spacing(um) Xeb '
read *,Xeb
print *,'input the DC Beta '
read *,Beta
vs = 2e7
deltaEg = 0.374
print *,'input the conduction-band off-set(Volts) deltaEc'
read *,deltaEc
deltaEv = 0.224
print *,'input the collector current(ma) Ic'
read *,Ic
print *,'input the collector voltage(V) Vce'
read *,Vce
taue =((We*100)**2/(2*Dpe))*((Dpe*Nab*Wb)/(Dnb*Nde*We))*exp(-deltaEc/Vt)
taub = (Wb*100)**2/(2*Dnb)  + (Wb*100)/vs
dc = 3.82e7*(Vce/Ndc)**0.5*1e-4
taucp = dc/(2*vs)
tauf = taue + taub + taucp
Cjc = 3.06e-9*(Ndc/Vce)**0.5*Ac*1e-15
Cje = 3.06e-9*(Nde/0.3)**0.5 * Ae*1e-15
gm = Ic/(Vt*1000)
tau1 = (Cje + Cjc + Cpad)/gm
Rec = rowCn/(Ae*1e-8)
Rebulk = (rowE1*We1*100 + rowE2*We2*100)/(Ae*1e-8)
Retot = Rec + Rebulk
Rc = (rowC*2e-5)/(Ae*1e-8)
tau2 = (Cjc+Cpad)*(Rc+Retot)
taut = tauf + tau1 + tau2
Ft = 1./(2*3.14159*taut)
rbi = rowIB*Se/(12*Le*5)
rbx = rowXB*Xeb/(10*Le)
rbc = (rowSK*Lt/(10*Le))*(1./tanh(Sb/Lt))
rb  = rbi + rbx + rbc
Fmax = (Ft/(8*3.14159*rb*(Cjc+Cpad)))**0.5
write(3,*)
write(3,*) 'RUN     ',RUN
write(3,*) 'We      ',We
write(3,*) 'We1     ',We1
write(3,*) 'We2     ',We2
write(3,*) 'Wb      ',Wb
write(3,*) 'Wc      ',Wc
```

```
write(3,*) 'Dpe     ',Dpe
write(3,*) 'Dnb     ',Dnb
write(3,*) 'upe     ',upe
write(3,*) 'unb     ',unb
write(3,*) 'Nde     ',Nde
write(3,*) 'Nab     ',Nab
write(3,*) 'Ndc     ',Ndc
write(3,*) 'rowE1   ',rowE1
write(3,*) 'rowE2   ',rowE2
write(3,*) 'rowIB   ',rowIB
write(3,*) 'rowXB   ',rowXB
write(3,*) 'rowC    ',rowC
write(3,*) 'rowCn   ',rowCn
write(3,*) 'rowCp   ',rowCp
write(3,*) 'rowSK   ',rowSK
write(3,*) 'Lt      ',Lt
write(3,*) 'Ae      ',Ae
write(3,*) 'Ac      ',Ac
write(3,*) 'Le      ',Le
write(3,*) 'Sb      ',Sb
write(3,*) 'Se      ',Se
write(3,*) 'Xeb     ',Xeb
write(3,*) 'Beta    ',Beta
write(3,*) 'deltaEc ',deltaEc
write(3,*) 'Ic      ',Ic
write(3,*) 'Vce     ',Vce
write(3,*) 'taue    ',taue
write(3,*) 'taub    ',taub
write(3,*) 'taucp   ',taucp
write(3,*) 'tauf    ',tauf
write(3,*) 'Cjc     ',Cjc
write(3,*) 'Cpad    ',Cpad
write(3,*) 'Cje     ',Cje
write(3,*) 'gm      ',gm
write(3,*) 'tau1    ',tau1
write(3,*) 'Rec     ',Rec
write(3,*) 'Rebulk  ',Rebulk
write(3,*) 'Re      ',Retot
write(3,*) 'Rc      ',Rc
write(3,*) 'tau2    ',tau2
write(3,*) 'taut    ',taut
write(3,*) 'Ft      ',Ft
write(3,*) 'rbi     ',rbi
write(3,*) 'rbx     ',rbx
write(3,*) 'rbc     ',rbc
write(3,*) 'rb      ',rb
write(3,*) 'Fmax    ',Fmax
go to 100
```

end

VITA

The author was born in West Palm Beach, Florida, December 5, 1952. He graduated from Castle High School in Kaneohe, Hawaii in 1970 and graduated from Linfield College in the spring of 1976 with a B.A. in Economics.

He worked as the assistant manager at Wickes Lumber in Richardson, Texas. He returned to the Portland area in 1979 and worked as a clothing salesman at the Lloyd Center Meier and Frank, while attending Portland State University. The author graduated in the spring of 1986 with a B.S. in Computer Engineering.

In September of 1986, he joined the graduate student staff at the Oregon Graduate Center while continuing to work at Meier and Frank. He was accepted into the Department of Applied Physics and Electrical Engineering and began his graduate studies that fall.

The following spring, he was awarded a stipend and became a full-time graduate student. That summer he worked at Wright-Patterson Air Base in Dayton, Ohio. As a summer-hire he created a program to de-embed S-parameter device data using the HP8510 network analyzer. He is currently with the High-Frequency-Component-Design Group at Tektronix, employed as the HP8510

System Manager and Component Engineer.

The author is married to Kathleen Mattern and has a set of five year old twin daughters and a new born child.